

OECD/NEA Nuclear Science Committee
Working Party on the Physics of Plutonium Fuels and Innovative Fuel Cycles

Physics of Plutonium Recycling

Volume IX

**Benchmark on Kinetic Parameters
in the CROCUS Reactor**

Evaluators

U. Kasemeyer, R. Früh, J.M. Paratte, R. Chawla
Paul Scherrer Institute, Switzerland

Internal Reviewer

J.M. Paratte

Independent Review

Benchmark participants (NEA WPPR)

K. Hesketh (BNFL), **Wolf Timm** (Framatome ANP),
E. Gomin, M. Kalugin, L. Maiorov (Kurchatov Institute), **E. Sartori** (OECD/NEA)

Independent Reviewers

Udo Wehmann (NEA Consultant), **Tsuyoshi Misawa** (RRI, U-Kyoto)

© OECD 2007
NEA No. 4440

NUCLEAR ENERGY AGENCY
ORGANISATION FOR ECONOMIC CO-OPERATION AND DEVELOPMENT

ORGANISATION FOR ECONOMIC CO-OPERATION AND DEVELOPMENT

The OECD is a unique forum where the governments of 30 democracies work together to address the economic, social and environmental challenges of globalisation. The OECD is also at the forefront of efforts to understand and to help governments respond to new developments and concerns, such as corporate governance, the information economy and the challenges of an ageing population. The Organisation provides a setting where governments can compare policy experiences, seek answers to common problems, identify good practice and work to co-ordinate domestic and international policies.

The OECD member countries are: Australia, Austria, Belgium, Canada, the Czech Republic, Denmark, Finland, France, Germany, Greece, Hungary, Iceland, Ireland, Italy, Japan, Korea, Luxembourg, Mexico, the Netherlands, New Zealand, Norway, Poland, Portugal, the Slovak Republic, Spain, Sweden, Switzerland, Turkey, the United Kingdom and the United States. The Commission of the European Communities takes part in the work of the OECD.

OECD Publishing disseminates widely the results of the Organisation's statistics gathering and research on economic, social and environmental issues, as well as the conventions, guidelines and standards agreed by its members.

* * *

This work is published on the responsibility of the Secretary-General of the OECD. The opinions expressed and arguments employed herein do not necessarily reflect the official views of the Organisation or of the governments of its member countries.

NUCLEAR ENERGY AGENCY

The OECD Nuclear Energy Agency (NEA) was established on 1st February 1958 under the name of the OEEC European Nuclear Energy Agency. It received its present designation on 20th April 1972, when Japan became its first non-European full member. NEA membership today consists of 28 OECD member countries: Australia, Austria, Belgium, Canada, the Czech Republic, Denmark, Finland, France, Germany, Greece, Hungary, Iceland, Ireland, Italy, Japan, Luxembourg, Mexico, the Netherlands, Norway, Portugal, Republic of Korea, the Slovak Republic, Spain, Sweden, Switzerland, Turkey, the United Kingdom and the United States. The Commission of the European Communities also takes part in the work of the Agency.

The mission of the NEA is:

- to assist its member countries in maintaining and further developing, through international co-operation, the scientific, technological and legal bases required for a safe, environmentally friendly and economical use of nuclear energy for peaceful purposes, as well as
- to provide authoritative assessments and to forge common understandings on key issues, as input to government decisions on nuclear energy policy and to broader OECD policy analyses in areas such as energy and sustainable development.

Specific areas of competence of the NEA include safety and regulation of nuclear activities, radioactive waste management, radiological protection, nuclear science, economic and technical analyses of the nuclear fuel cycle, nuclear law and liability, and public information. The NEA Data Bank provides nuclear data and computer program services for participating countries.

In these and related tasks, the NEA works in close collaboration with the International Atomic Energy Agency in Vienna, with which it has a Co-operation Agreement, as well as with other international organisations in the nuclear field.

© OECD 2007

No reproduction, copy, transmission or translation of this publication may be made without written permission. Applications should be sent to OECD Publishing: rights@oecd.org or by fax (+33-1) 45 24 99 30. Permission to photocopy a portion of this work should be addressed to the Centre Français d'exploitation du droit de Copie (CFC), 20 rue des Grands-Augustins, 75006 Paris, France, fax (+33-1) 46 34 67 19, (contact@cfcopies.com) or (for US only) to Copyright Clearance Center (CCC), 222 Rosewood Drive Danvers, MA 01923, USA, fax +1 978 646 8600, info@copyright.com.

Cover credit: École polytechnique fédérale de Lausanne.

FOREWORD

The OECD/NEA Working Party on the Physics of Plutonium Fuels and Innovative Fuel Cycles (WPPR) was established in 1993 and reports to the OECD/NEA Nuclear Science Committee. Its main activity has been to analyse benchmarks carried out to answer technical questions related to the physics of plutonium fuels. Past volumes of published work have examined the physics of plutonium-fuelled pressurised water reactors (PWRs) and boiling water reactors (BWRs), as well as the physics of metal- and oxide-fuelled fast reactors. The present report concentrates on plutonium-fuelled, high-temperature reactors (HTRs). This activity was taken over and expanded by a new Working Party on Scientific Issues in Reactor Systems (WPRS).

Most of the previous studies were devoted to benchmarks on the static behaviour of different reactor configurations or evolution of isotopic inventories. The need for an experimental benchmark relative to reactor kinetics parameters became evident. However, no experimental data for kinetic parameters in MOX cores were generally available, thus the decision was taken to use a UO₂-fuelled core for validating the codes with the possibility of later adding a computational benchmark with MOX fuel loading. The present report concerns experiments carried out at the *Institut de génie atomique* (IGA) of the *École polytechnique fédérale de Lausanne* (EPFL) operating the zero-power research reactor CROCUS, which is mainly used for teaching purposes.

The reactor period was measured in the CROCUS reactor for several different delayed super-critical conditions. Two types of reactivity changes were measured employing an appropriate stable period technique in each case. The first series of experiments involved increasing the water level above the critical level. The second series was carried out by inserting/removing one of the absorber rods into/out of the core.

This reactor physics benchmark is included in the International Reactor Physics Experiments Handbook (IRPhE) published by the OECD/NEA on DVD (see www.nea.fr/html/dbprog/IRPhE-latest.htm for further details).

The *Physics of Plutonium Recycling* series currently comprises the following titles:

- *Volume I: Issues and Perspectives* (OECD/NEA, 1995).
- *Volume II: Plutonium Recycling in Pressurised Water Reactors* (OECD/NEA, 1995).
- *Volume III: Void Reactivity Effect in Pressurised Water Reactors* (OECD/NEA, 1995).
- *Volume IV: Fast Plutonium Burner Reactors: Beginning of Life* (OECD/NEA, 1995).
- *Volume V: Plutonium Recycling in Fast Reactors* (OECD/NEA, 1996).
- *Volume VI: Multiple Plutonium Recycling in Advanced PWRs* (OECD/NEA, 2002).
- *Volume VII: BWR MOX Benchmark – Specification and Results* (OECD/NEA, 2003).
- *Plutonium Management in the Medium Term – A Review by the OECD/NEA Working Party on the Physics of Plutonium Fuels and Innovative Fuel Cycles (WPPR)*, (OECD/NEA, 2003).
- *Pressurised Water Reactor MOX/UO₂ Core Transient Benchmark* (OECD/NEA, 2006).
- *Volume VIII: Results of a Benchmark Considering a High-temperature Reactor (HTR) Fuelled with Reactor-grade Plutonium* (OECD/NEA, 2007).

TABLE OF CONTENTS

Foreword	3
Status of compilation/evaluation/peer review	7
Chapter 1 DETAILED DESCRIPTION	9
1.1 Description of the critical and/or subcritical configuration	10
1.1.1 Overview of experiment.....	10
1.1.2 Geometry of the experiment configuration and measurement procedure	10
1.1.3 Material data.....	20
1.1.4 Temperature information.....	21
1.1.5 Additional information relevant to critical and subcritical measurements	21
1.2 Description of buckling and extrapolation length measurements.....	21
1.3 Description of spectral characteristics measurements	21
1.4 Description of reactivity effects measurements.....	21
1.5 Description of reactivity coefficient measurements	21
1.6 Description of kinetics measurements	22
1.6.1 Overview of experiment.....	22
1.6.2 Geometry of the experiment configuration and measurement procedure	22
1.6.3 Material data.....	28
1.6.4 Temperature data.....	28
1.6.5 Additional information relevant to kinetics measurements	28
1.7 Description of reaction rate distribution measurements	28
1.8 Description of power distribution measurements	28
1.9 Description of isotopic measurements.....	29
1.10 Description of other miscellaneous types of measurements.....	29
Chapter 2 EVALUATION OF EXPERIMENTAL DATA	31
2.1 Evaluation of the critical and/or subcritical configuration data.....	31
2.1.1 Inaccuracies for the fuel densities	31
2.1.2 About the content of ²³⁴ U	31
2.1.3 Inaccuracies of the non-fuel materials.....	32
2.1.4 Effect of the configuration data inaccuracies on the reactivity	33
2.1.5 Summary of the effects of the configuration data inaccuracies on the reactivity	36
2.2 Evaluation of buckling and extrapolation length data	37
2.3 Evaluation of spectral characteristics data.....	37
2.4 Evaluation of reactivity effects data	37
2.5 Evaluation of reactivity coefficient data.....	37
2.6 Evaluation of kinetics measurement data	37
2.7 Evaluation of reaction rate distributions.....	37
2.8 Evaluation of power distribution data.....	38

2.9	Evaluation of isotopic measurements	38
2.10	Evaluation of other miscellaneous types of measurements	38
Chapter 3	BENCHMARK SPECIFICATIONS	39
3.1	Benchmark model specifications for critical and/or subcritical measurements	39
3.1.1	Description of the benchmark model simplifications.....	39
3.1.2	Dimensions.....	40
3.1.3	Material data.....	45
3.1.4	Temperature of materials.....	46
3.1.5	Experimental and benchmark model k_{eff} and/or subcritical parameters	46
3.2	Benchmark model specifications for buckling and extrapolation-length measurements	46
3.3	Benchmark model specifications for spectral characteristics measurements	46
3.4	Benchmark model specifications for reactivity effects measurements.....	47
3.5	Benchmark model specifications for reactivity coefficient measurements	47
3.6	Benchmark model specifications for kinetics measurements.....	47
3.6.1	Description of the benchmark model simplifications.....	47
3.6.2	Dimensions.....	48
3.6.3	Material data.....	48
3.6.4	Temperature data.....	48
3.6.5	Experimental and benchmark model kinetics measurements.....	48
3.7	Benchmark model specifications for reaction rate distribution measurements	49
3.8	Benchmark model specifications for power distribution measurements	49
3.9	Benchmark model specifications for isotopic measurements.....	49
3.10	Benchmark model specifications for other miscellaneous types of measurements	49
Chapter 4	RESULTS OF SAMPLE CALCULATIONS	51
4.1	Results of calculations of the critical or subcritical configurations.....	51
4.2	Results of buckling and extrapolation length calculations	51
4.3	Results of spectral characteristics calculations.....	51
4.4	Results of reactivity effects calculations	52
4.5	Results of reactivity coefficient calculations.....	52
4.6	Results of kinetics parameter calculations.....	52
4.6.1	Calculated kinetics parameters for Case 1 ($H_1 = H_{\text{crit}}$)	52
4.6.2	Calculated reactivity effects	53
4.6.3	“Kinetics” reactivity effects	54
4.7	Results of reaction rate distribution calculations.....	56
4.8	Results of power distribution calculations.....	56
4.9	Results of isotopic calculations	56
4.10	Results of calculations for other miscellaneous types of measurements	56
	References	57
	Appendix A Computer codes, cross-sections and typical input listings	59
	Appendix B Measurement protocols.....	77

Status of compilation/evaluation/peer review

Section 1		Compiled	Independent review	Working group review	Approved
1.0	DETAILED DESCRIPTION	YES	YES	YES	YES
1.1	Description of the critical and/or subcritical configuration	YES	YES	YES	YES
1.2	Description of buckling and extrapolation length measurements	NA	NA	NA	NA
1.3	Description of spectral characteristics measurements	NA	NA	NA	NA
1.4	Description of reactivity effects measurements	NA	NA	NA	NA
1.5	Description of reactivity coefficient measurements	NA	NA	NA	NA
1.6	Description of kinetics measurements	YES	YES	YES	YES
1.7	Description of reaction-rate distribution measurements	NA	NA	NA	NA
1.8	Description of power distribution measurements	NA	NA	NA	NA
1.9	Description of isotopic measurements	NA	NA	NA	NA
1.10	Description of other miscellaneous types of measurements	NA	NA	NA	NA
Section 2		Evaluated	Independent review	Working group review	Approved
2.0	EVALUATION OF EXPERIMENTAL DATA	YES	YES	YES	YES
2.1	Evaluation of critical and/or subcritical configuration data	YES	YES	YES	YES
2.2	Evaluation of buckling and extrapolation length data	NA	NA	NA	NA
2.3	Evaluation of spectral characteristics data	NA	NA	NA	NA
2.4	Evaluation of reactivity effects data	NA	NA	NA	NA
2.5	Evaluation of reactivity coefficient data	NA	NA	NA	NA
2.6	Evaluation of kinetics measurements data	YES	YES	YES	YES
2.7	Evaluation of reaction rate distributions	NA	NA	NA	NA
2.8	Evaluation of power distribution data	NA	NA	NA	NA
2.9	Evaluation of isotopic measurements	NA	NA	NA	NA
2.10	Evaluation of other miscellaneous types of measurements	NA	NA	NA	NA

Status of compilation/evaluation/peer review (cont.)

Section 3	Complied	Independent review	Working group review	Approved
3.0 BENCHMARK SPECIFICATIONS	YES	YES	YES	YES
3.1 Benchmark model specifications for critical and/or subcritical measurements	YES	YES	YES	YES
3.2 Benchmark model specifications for buckling and extrapolation length measurements	NA	NA	NA	NA
3.3 Benchmark model specifications for spectral characteristics measurements	NA	NA	NA	NA
3.4 Benchmark model specifications for reactivity effects measurements	NA	NA	NA	NA
3.5 Benchmark model specifications for reactivity coefficient measurements	NA	NA	NA	NA
3.6 Benchmark model specifications for kinetics measurements	YES	YES	YES	YES
3.7 Benchmark model specifications for reaction-rate distribution measurements	NA	NA	NA	NA
3.8 Benchmark model specifications for power distribution measurements	NA	NA	NA	NA
3.9 Benchmark model specifications for isotopic measurements	NA	NA	NA	NA
3.10 Benchmark model specifications of other miscellaneous types of measurements	NA	NA	NA	NA
Section 4	Compiled	Independent review	Working group review	Approved
4.0 RESULTS OF SAMPLE CALCULATIONS	YES	YES	YES	YES
4.1 Results of calculations of the critical or subcritical configurations	YES	YES	YES	YES
4.2 Results of buckling and extrapolation length calculations	NA	NA	NA	NA
4.3 Results of spectral characteristics calculations	NA	NA	NA	NA
4.4 Results of reactivity effect calculations	NA	NA	NA	NA
4.5 Results of reactivity coefficient calculations	NA	NA	NA	NA
4.6 Results of kinetics parameter calculations	YES	YES	YES	YES
4.7 Results of reaction-rate distribution calculations	NA	NA	NA	NA
4.8 Results of power distribution calculations	NA	NA	NA	NA
4.9 Results of isotopic calculations	NA	NA	NA	NA
4.10 Results of calculations of other miscellaneous types of measurements	NA	NA	NA	NA
Section 5	Compiled	Independent review	Working group review	Approved
5.0 REFERENCES	YES	YES	YES	YES
Appendix A: Computer codes, cross-sections and typical input listings	YES	YES	YES	YES
Appendix B: Measurement protocols	YES	YES	YES	YES

IDENTIFICATION NO.: CROCUS-LWR-RESR-001
CRIT-KIN

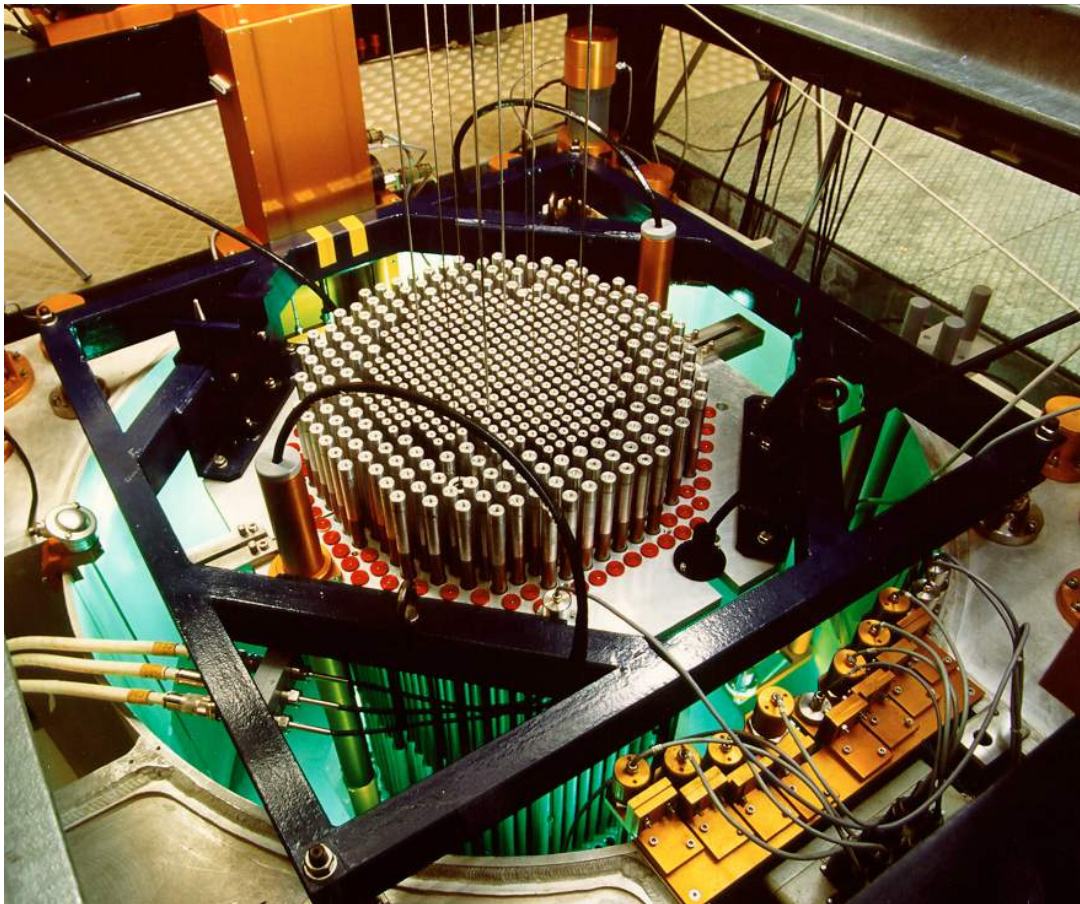
KEY WORDS: kinetics parameters, light water moderator, reactor period, square lattice, UO₂, uranium-metal, water-level variation, zero-power critical facility

Chapter 1
DETAILED DESCRIPTION

The CROCUS reactor, operated by the Swiss Federal Institute of Technology, Lausanne [1], is a simple two-zone uranium-fuelled, H₂O-moderated critical research facility. Figure 1.1 gives a view of the facility, a so-called *zero power* reactor, with a maximum allowed power of 100 W. The core is approximately cylindrical in shape with a diameter of about 60 cm and a height of 100 cm.

In 1995, in the CROCUS reactor a configuration with a central zone of 1.806 wt.%-enriched UO₂ rods and an outer zone of 0.947 wt.%-enriched uranium metal rods was made critical by raising the water level. Later on, the reactor was used for different experiments. Some configurations are evaluated here and are approved as benchmark configurations for the reactivity difference between the critical water level and some supercritical conditions.

Figure 1.1. View of the CROCUS reactor of the Swiss Federal Institute of Technology, Lausanne



1.1 Description of the critical and/or subcritical configuration

1.1.1 Overview of experiment

Two different kinds of measurements were carried out in the CROCUS reactor:

- a) Variation of the water moderator level. For this type of configuration, four different water levels were measured, one for the critical state (i.e. when the inverse reactor period is zero) and three higher water levels for supercritical states.
- b) Insertion of an absorber rod, adjustment of the water level to the new critical height, and then removal of the absorber rod. For this second set of experiments, a total of four configurations were measured, two for the critical states with the absorber rod inserted and two supercritical states obtained after withdrawing the absorber rod [2].

The experiments at different water levels were performed in 1996 and those with absorber rods in 1997.

Notice: The uncertainties or inaccuracies given represent experimental standard deviations of 1σ .

1.1.2 Geometry of the experiment configuration and measurement procedure

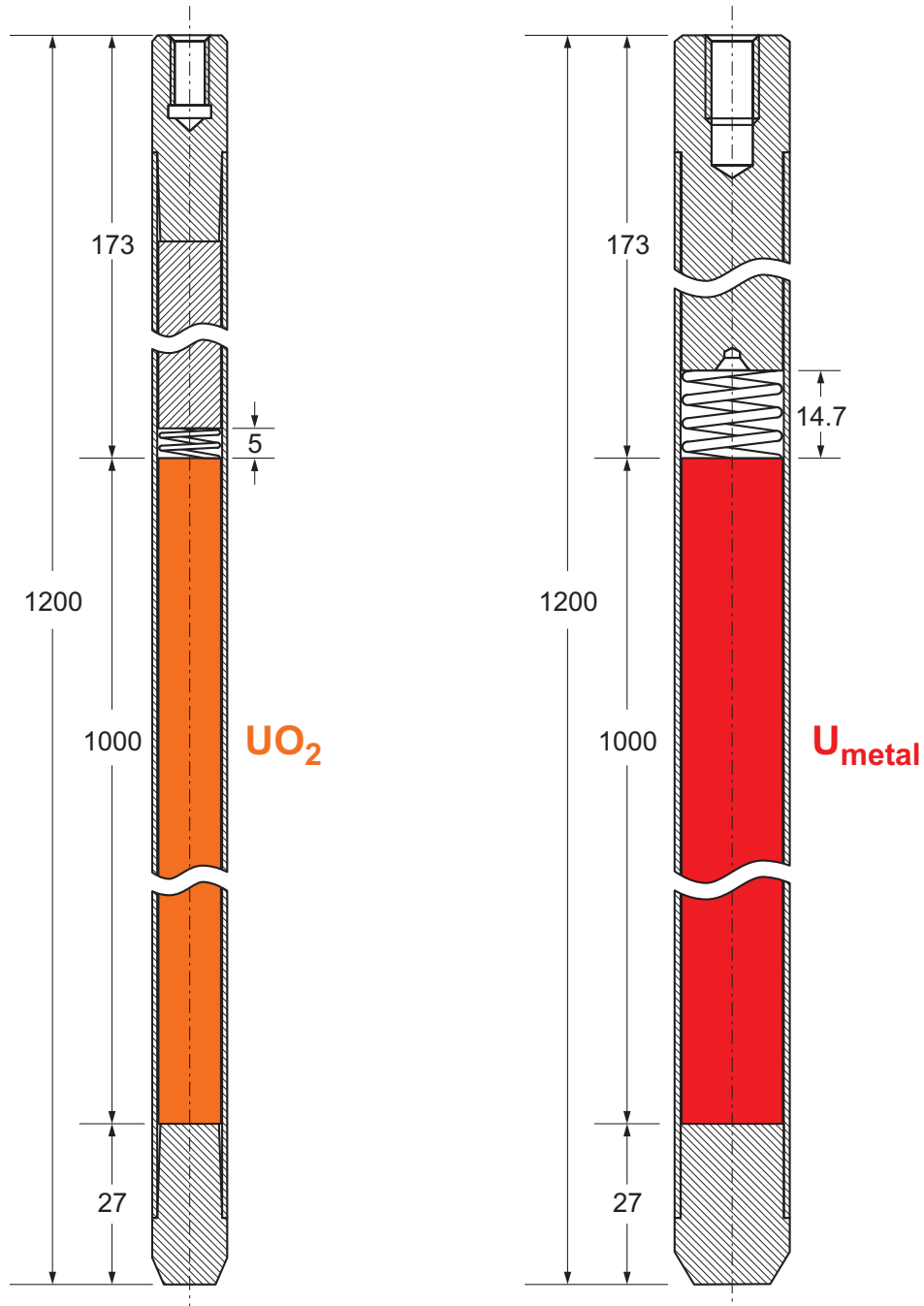
Axial arrangement

The reactivity in the CROCUS reactor is controlled by the water level, which can be adjusted with an accuracy of ± 0.1 mm or ~ 0.4 pcm. The maximum water height is 100 cm, while the critical water height for the reference configuration with 172 metallic uranium rods according to Figure 1.4 (without absorber rods) was measured to be 96.51 ± 0.01 cm. Figures 1.2 and 1.3 depict axial sections of the CROCUS reactor. The core is bound axially by an upper and a lower grid plate. Both grid plates incorporate a cadmium layer with a thickness of 0.50 ± 0.05 mm to limit the axial thermal flux. The active fuel length starts at the top surface of the lower cadmium layer and extends to 100 cm. The uncertainty of the position of the lower end of the fuel columns against the top surface of the lower Cd layer does not exceed ± 0.1 mm. The main geometrical data in axial direction are given in Table 1.1.

Table 1.1. Thickness of axially partitioned structure materials [mm]

Parameter	Dimension [mm]
Base plate	30.0 ± 0.1
Lower grid a	5.0 ± 0.1
Lower Cd plate	0.50 ± 0.05
Lower grid b (Lgb)	5.0 ± 0.1
Distance between Lgb and Uga	1000 ± 0.2
Upper grid a (Uga)	5.0 ± 0.1
Upper Cd plate	0.50 ± 0.05
Upper grid b	15.0 ± 0.1
Upper part of rods	147.5 ± 0.5

Figure 1.2. Axial sections of the two fuel rod types used in the CROCUS reactor



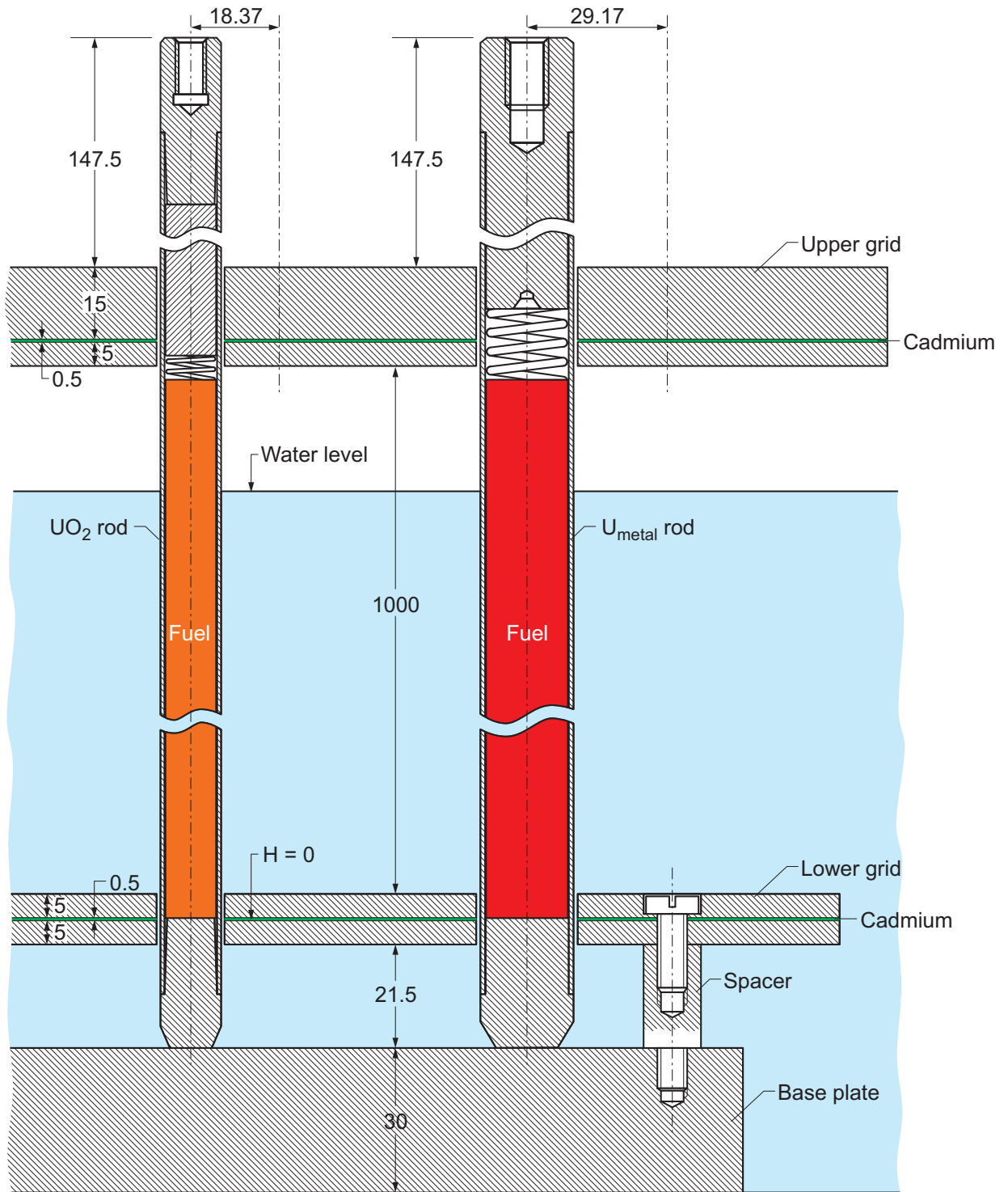
Cladding thickness: 0.85 mm
 External cladding diameter: 12.60 mm
 Fuel diameter: 10.52 mm
²³⁵U weight fraction: 1.806%
 Cladding material: Aluminum

Cladding thickness: 0.975 mm
 External cladding diameter: 19.3 mm
 Fuel diameter: 17.0 mm
²³⁵U weight fraction: 0.947%
 Cladding material: Aluminum

Dimensions in mm

07-GA50013-38-1

Figure 1.3. Axial section depicting various components of the CROCUS reactor



Dimensions in mm

07-GA50013-38-2

Radial arrangement

Figure 1.4 shows the radial or X-Y distribution of the fuel rods for the reference core configuration with 336 UO₂ rods and 172 metallic U rods. This configuration has an eight-fold symmetry for both fuel zones, while for the measurements with the absorber rods the configuration shown in Figure 1.5 was used, in which the metallic fuel zone (with 176 instead of 172 rods) has only a two-fold symmetry. Because of the different pitches used, the two fuel zones are separated by water gaps, as indicated in Figures 1.4 and 1.5. The outer fuel zone is surrounded by a water reflector with an outer radius of 65 cm. The vessel wall consisting of aluminium has a thickness of 1.2 cm. Figures 1.6 through 1.8 show the upper, the lower and the base plates, respectively.

The gap between the two halves of the upper grid plate (Figure 1.6) is 5 mm. At both ends of the gap two stirrups made of stainless steel stiffly fix the two half-grids together (the two stirrups can be seen on Figure 1.1). As they are axially located above the water level and radially well out of the reactor core, they have no influence on the reactivity of the reactor.

Fuel rods

As mentioned, there are two different kinds of fuel rods within the two fuel zones of the CROCUS reactor. The central zone is fuelled with 336 uranium dioxide fuel rods, which are thinner rods with a square lattice pitch of 1.8370 ± 0.0002 cm. The peripheral zone is loaded with 172 (176 in the cases of absorber rods) thicker metallic uranium fuel rods with a pitch of 2.9170 ± 0.0002 cm. All other parameters for the two types of fuel rods are given in Figures 1.2 and 1.3. All fuel rods have an aluminium cladding and are maintained in a vertical position by the upper grid and lower grid plates spaced 100 cm apart (see Figures 1.6 and 1.7). The core is located in a water tank of 130 cm diameter. De-ionised water (H₂O) acts as moderator and reflector.

The fuel rod data are collected in Table 1.2.

Table 1.2. Fuel rod data for the CROCUS reactor

Parameter	Unit	UO ₂	U _{metal}
Cladding thickness	mm	0.85±0.05	0.975±0.05
External cladding diameter	mm	12.60±0.1	19.3+0.1/-0.0
Fuel diameter	mm	10.520±0.017	17.00±0.02
²³⁵ U enrichment	wt. %	1.8060±0.0007	0.9470±0.0007
Square pitch	mm	18.370±0.002	29.170±0.002
Fuel density	g/cm ³	10.556±0.034 ^(a)	18.677±0.044 ^(a)

^(a) This uncertainty was not measured but calculated on the basis of fuel mass and volume, Section 2.1.1.

Absorber rods

For the measurements with neutron absorber rods, two such rods were inserted, one at a time, in the centre of the core (i.e. in a position at the middle of the four centrally located UO₂ fuel rods; see Figures 1.5 and 1.6). They were clad in cylindrical aluminium tubes with an outer diameter of $8.0 \pm 0.1 / -0.0$ mm and a wall thickness of 1.00 ± 0.05 mm. The first rod was filled with water which contained 6768 ± 0.1 ppm natural boron (natural isotopic composition, H₂O at 20°C and 0.1 MPa). The second rod contained pellets with $3.72 \pm 1.0\%$ g/cm³ ZrO₂ and $0.874 \pm 1.0\%$ g/cm³ Er₂O₃.

(i.e. $0.764 \pm 1.0\%$ g/cm³ Er). Each pellet was measured in height and diameter with an accuracy of ± 0.01 mm, and weighed with an accuracy of ± 0.0001 g. The average diameter of these pellets is obtained as $5.89 \pm 0.2\%$ mm.

In the axial direction, the absorber column starts at the position 0.0 ± 0.1 mm. The height of the absorber column is 100.0 cm for the boron rod and 100.93 cm for the Er rod. The total height of the Al tube (outer/inner diameter of 8.0/6.0 mm), containing the absorbers, is 1 300 mm. Above the absorber columns the tube is empty, filled with air. The accuracy of these heights is not known (but it has no influence on the multiplication factor of the corresponding configuration because it is located well above the water level).

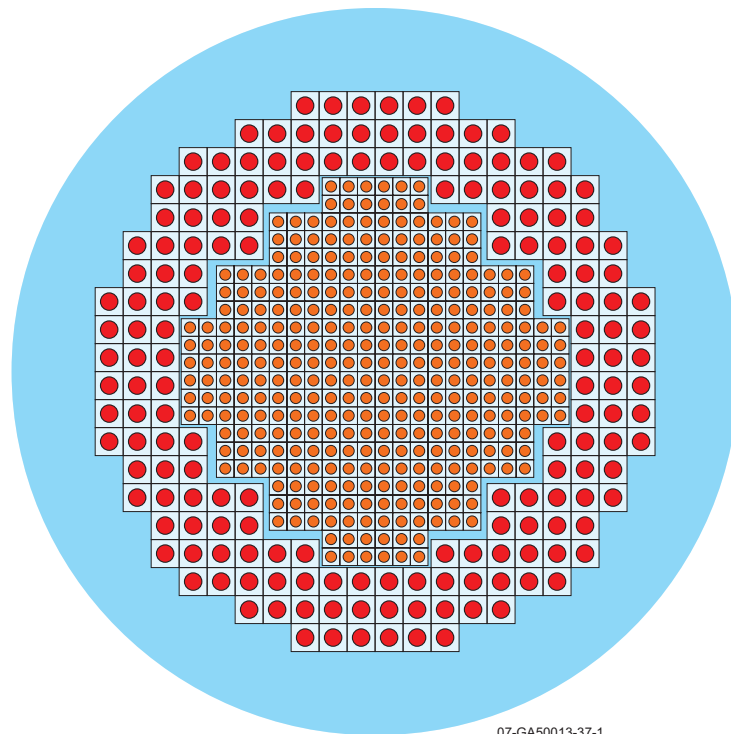
The absorber rod data are collected in Table 1.3. About the Er pellets: 105 pellets were measured for their diameter, length and mass. The results are: mean diameter = 5.878 ± 0.008 mm, mean height = 9.61 ± 0.17 mm, mean mass = 1.171 ± 0.023 g.

Table 1.3. Absorber rod data for the CROCUS reactor

Parameter	Unit	Dimension
Outer diameter	mm	$8.0 + 0.1 / - 0.0$
Wall thickness	mm	1.00 ± 0.05
Absorber B _{nat} : density	ppm in water at 20°C	$6\,768 \pm 0.1\%$
Absorber Er: density	g/cm ³	$4.594 \pm 1\%$
Absorber Er: pellet diameter	mm	$5.89 \pm 0.2\%$

The critical water levels for the absorber cases were 96.92 ± 0.01 cm for the boron rod and 98.63 ± 0.01 cm for the erbium rod.

Figure 1.4. Distribution of the two different fuel rod types in the CROCUS reactor for the measurements with variation of the water level







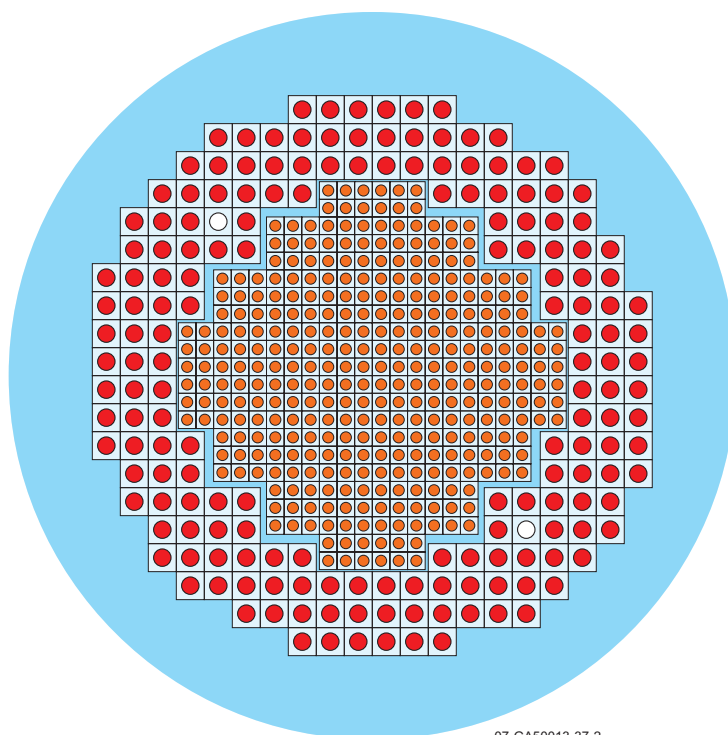
-  336 UO_2 cells (square lattice with 18.37 mm pitch)
-  Water gap (space between UO_2 and U_{metal} cells)
-  172 U_{metal} cells (square lattice with 29.17 mm pitch)
-  Water reflector (external radius 65 cm)

Figure 1.5. Distribution of the two different fuel rod types in the CROCUS reactor for the measurements with the absorber rods



07-GA50013-37-2






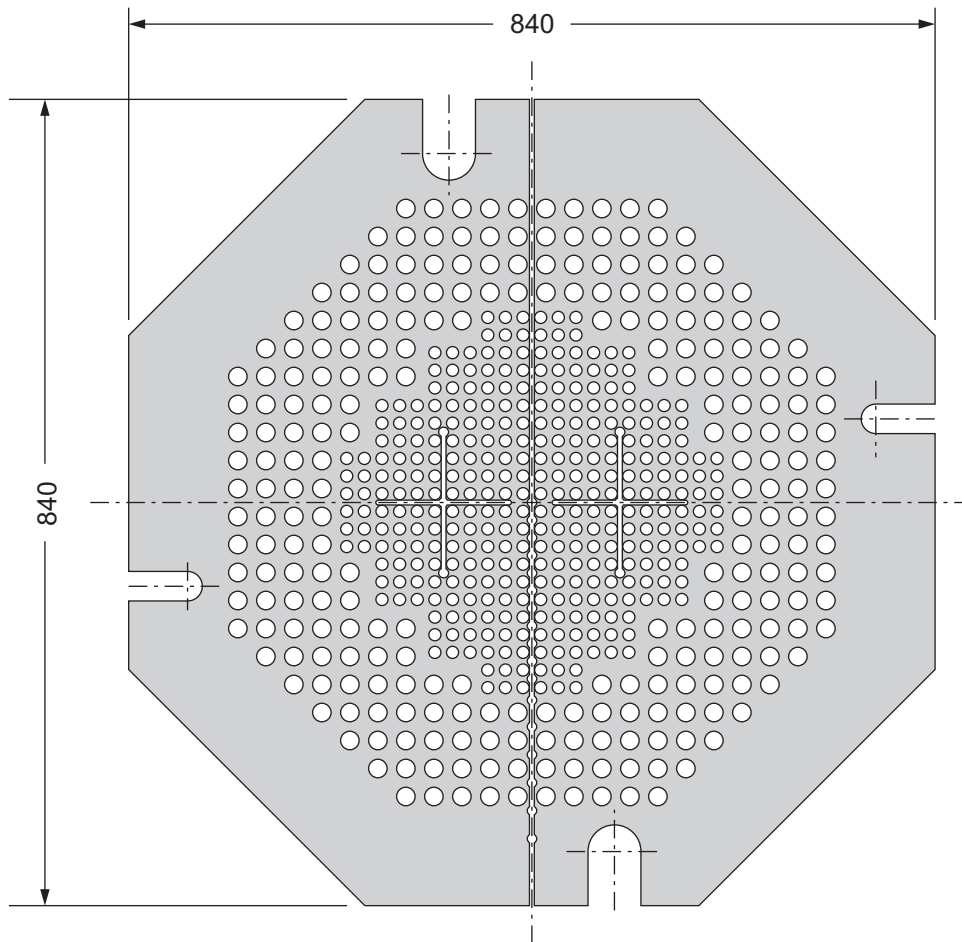
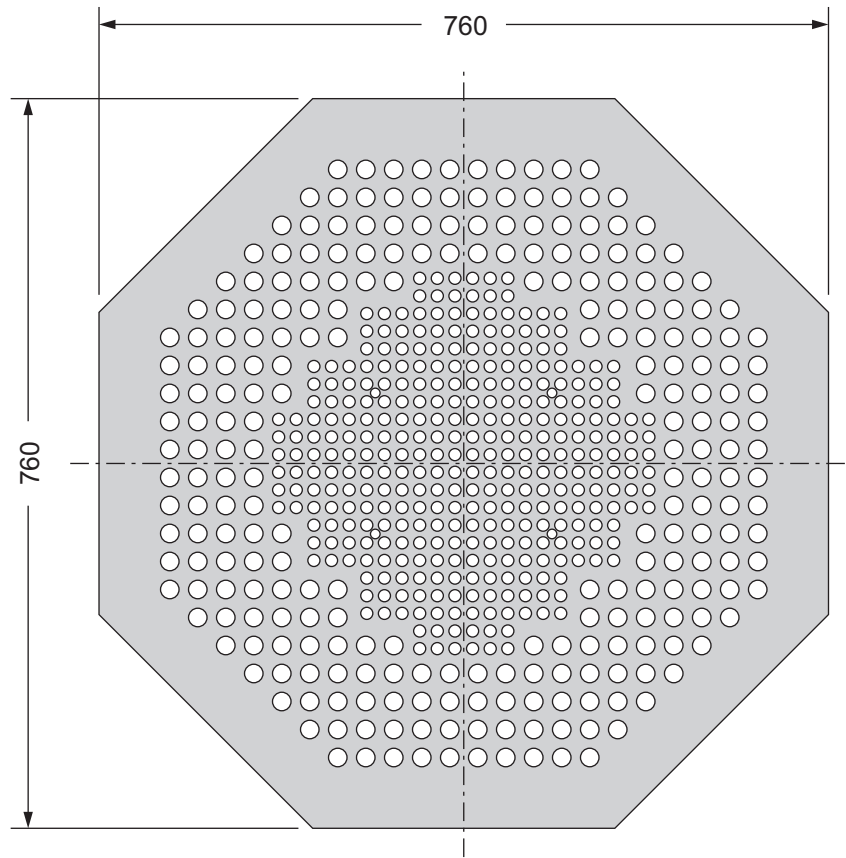
-  336 UO_2 cells (square lattice with 18.37 mm pitch)
-  Water gap (space between UO_2 and U_{metal} cells)
-  176 U_{metal} cells (square lattice with 29.17 mm pitch)
-  Water reflector (external radius 65 cm)
-  Same as U_{metal} cell but without uranium (empty, i.e. air filled, Al tube)

Figure 1.6. Upper grid plate of CROCUS (dimensions in mm)



07-GA50013-37-3

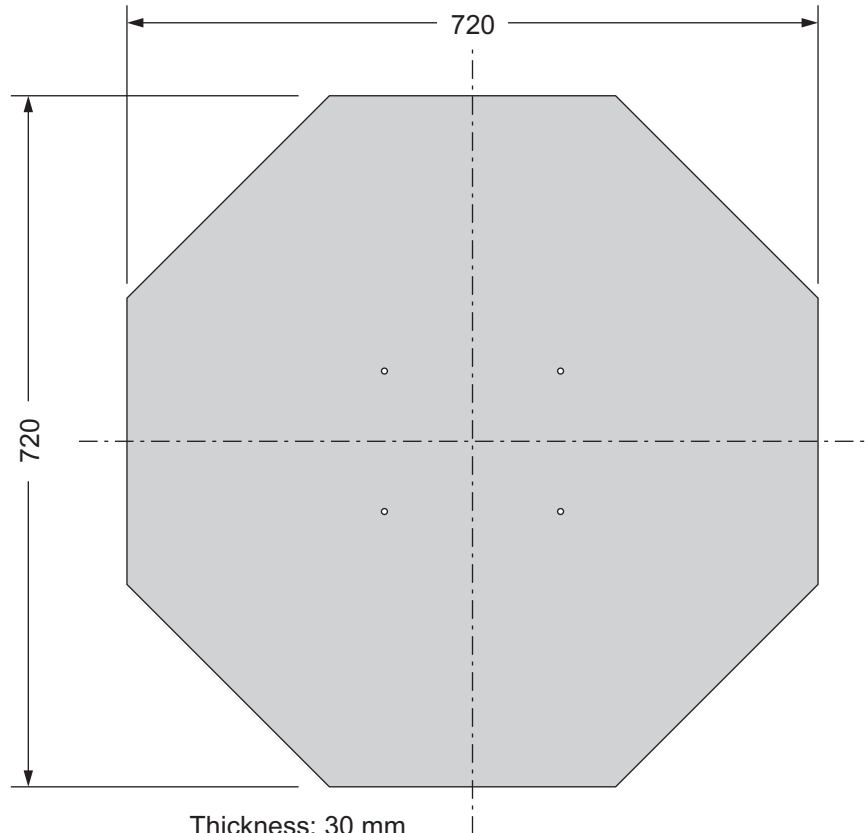
Figure 1.7. Lower grid plate of CROCUS (dimensions in mm)



Dimensions in mm

07-GA50013-37-4

Figure 1.8. Base plate of CROCUS (dimensions in mm)



Dimensions in mm

07-GA50013-37-5

1.1.3 Material data

Fuel rods

As mentioned, two different kinds of fuel rods are used within the two fuel zones of the CROCUS reactor. The central zone is loaded with uranium dioxide fuel rods enriched to 1.8060 ± 0.0007 wt.% ^{235}U with a density of 10.556 ± 0.034 g/cm³. The peripheral zone is loaded with metallic uranium fuel rods that are enriched to 0.9470 ± 0.0007 wt.% with a density of 18.677 ± 0.044 g/cm³ (*Notice: The uncertainties on the fuel density were not measured but calculated on the basis of fuel mass and volume, Section 2.1*). All fuel rods have an aluminium cladding.

The total burn-up accumulated during the reactor operation is 3 930 W·h for the UO₂ fuel and 4 910 W h for the metallic uranium. If it is assumed that all the power is produced by fissions in ^{235}U , the total number of fissions in the UO₂ fuel is $4.42\text{E}+17$, and it is $5.52\text{E}+17$ in the metallic uranium. The total number of ^{235}U atoms is $5.06\text{E}+25$ in the UO₂ fuel and $5.32\text{E}+25$ in the metallic uranium. Therefore, the relative reduction of the number of ^{235}U atoms due to the burn-up is $1.1\text{E}-8$ for the UO₂ fuel and $1.0\text{E}-8$ in the metallic uranium, which is negligible. It can therefore be assumed that the fuel has not accumulated any burn-up.

The fuel rods are filled with helium at a pressure 0.1 MPa. The core is located in a water tank containing de-ionised water (H₂O) as the moderator and reflector.

As confirmation of the data given here, some measurement protocols were added to this report as appendices:

- Appendix B.1: Measurement of the enrichment of the UO₂ fuel pellets;
- Appendix B.2: Measurement of the masses of the UO₂ fuel rods;
- Appendix B.3: Measurement of the dimensions and masses of the metallic U fuel rods.

Non-fuel materials

The non-fuel materials are listed in Table 1.4.

Table 1.4. Description of non-fuel materials in the CROCUS reactor ^(a)

Name	Material	Density [g/cm ³]
Base plate Lower & upper grids End plugs Cladding	Aluminium	2.70
Cadmium layers	Cadmium	8.65
Screws Springs	Fe/Cr/Ni/Mn 70.35/19.15/8.50/2.00 at.%	7.82 ^(b)
Moderator	Water	0.99823 ^(c)
Filler gas (fuel rods)	Helium	1.64E-4 ^(c)
Air above water level	Air	1.2047E-3 ^(c)

^(a) For the evaluation of the effect of possible uncertainties, see Section 2.1.

^(b) Best estimate.

^(c) Taken from Ref. [3].

Absorber rods

As mentioned, two neutron absorber rods were inserted, one at a time, in the centre of the core. The absorber rods were clad in cylindrical aluminium tubes. The first rod was filled with water which contained $6768 \pm 0.1\%$ ppm natural boron. The second rod contained pellets with $3.72 \pm 1.0\%$ g/cm^3 ZrO_2 and $0.874 \pm 1.0\%$ g/cm^3 Er_2O_3 (i.e. $0.764 \pm 1.0\%$ g/cm^3 Er).

1.1.4 Temperature information

The temperature of all materials is $20.00 \pm 0.02^\circ\text{C}$. Water continuously runs between the reactor vessel and an auxiliary vessel. The water temperature is measured at three different levels in the reactor vessel.

1.1.5 Additional information relevant to critical and subcritical measurements

Most of the data given above were measured several times, and the values shown represent, in each case, a mean overall measurements done for a given data item. In Table 1.2, the various data are given together with their inaccuracies representing experimental standard deviation (1σ). The fuel pellets were made exactly cylindrical by polishing; the fuel column height of each rod was adjusted to be between 1000.0 and 1000.8 mm. Afterwards, each fuel rod was measured and weighed, and the fuel density was derived as a mean value over all individual measurements.

The density of water was not measured but taken from Ref. [3]. Its inaccuracy is included in that of the temperature ($\pm 0.02^\circ\text{C}$, corresponding to 1σ).

For the densities of Al, Cd and steel, no inaccuracies could be obtained through direct measurements.

1.2 Description of buckling and extrapolation length measurements

Buckling and extrapolation length measurements were not performed.

1.3 Description of spectral characteristics measurements

Spectral characteristics measurements were not performed.

1.4 Description of reactivity effects measurements

Reactivity effects measurements were not performed.

1.5 Description of reactivity coefficient measurements

Reactivity coefficient measurements were not performed.

1.6 Description of kinetics measurements

1.6.1 Overview of experiment

The goal of the experiments was to determine the reactor period for different supercritical states. These were achieved by two types of measurements:

- a) Increasing the water level: The critical configuration containing 172 metallic U fuel rods (Figure 1.4) was made critical by adjusting the water level. The water level was then raised up, the reactor becoming supercritical. After some time (30-40 sec) in order to allow for the transients to vanish, the flux increases exponentially. The time variation of the flux curve was measured with a multi-channel analyser, and the inverse reactor period was determined from the slope of the flux curve. One critical configuration (denoted H_1), where the inverse reactor period is zero, and three supercritical ones were measured in that way.
- b) Withdrawing an absorber rod: For these experiments, the configuration with 176 metallic U fuel rods was used (Figure 1.5). First, an absorber rod containing either borated water or zirconium-erbium pellets was located at the very centre of the configuration, between the four central UO_2 rods. With the absorber rod inserted, the reactor was made critical by adjusting the water level. Afterwards, the absorber rod was withdrawn, the water level being kept constant. Therefore, the reactor became supercritical, and the slope of the flux curve was measured in the same way as for Case A. Two critical configurations with an absorber rod inserted and two supercritical configurations after withdrawing the absorber rod were measured.

The following sections describe the material and geometrical data used for these measurements.

1.6.2 Geometry of the experiment configuration and measurement procedure

For the measurements with *variation of the water level*, the radial partition of the materials is shown in Figure 1.4. With 172 metallic U fuel rods, this configuration has an eight-fold symmetry for both fuel zones.

For the measurements with an *absorber rod at the centre* of the UO_2 fuel zone, the configuration shown in Figure 1.5 was used; it counts 176 metallic U fuel rods, and it has only a two-fold symmetry. The absorber rods consist of an Al tube with an outer diameter of $8.0+0.1/-0.0$ mm and a wall thickness of 1.00 ± 0.05 mm. The borated water radially fills the entire volume of the rod. The Zr-Er pellets have an outer diameter of $5.89\pm 0.2\%$ mm. In the axial direction, the absorber column starts at the position 0.0 ± 0.1 mm. The total height is 100.0 cm for the boron rod and 100.93 cm for the Er rod. The tolerance of these heights is not known.

The axial partition of the materials in the reactor core is shown in Figures 1.2 and 1.3 for the two fuel zones and for the structure materials. It is the same for all configurations measured.

A permanent water flow circulates between the reactor tank and an auxiliary tank. A variable overflow plate determines the exit height from the reactor tank. In this way, the water level in the reactor tank can be adjusted continuously between $H = 80$ cm and $H = 100$ cm. The reference level $H = 0$ is determined by the base of the uranium column in the core; it is the same position (with an accuracy of ± 0.1 mm) as the top surface of the lower Cd plate.

The kinetics measurements carried out here are based on the so-called “stable period method”. The point kinetics model [5] is used to determine the reactivity through measurement of the stable reactor period. The neutron population $P(t)$ and the precursor nuclide density $C_i(t)$ in each precursor group are governed by the two following equations:

$$\frac{dP}{dt} = \frac{(1-\beta)k_e(t)-1}{\ell(t)} P(t) + \sum_i \lambda_i C_i(t) \quad (1)$$

$$\frac{dC_i}{dt} + \lambda_i C_i(t) = \beta_i \frac{k_e}{\ell(t)} P(t) \quad (2)$$

where: $\beta = \sum_i \beta_i$ Delayed neutron fraction

λ_i Decay constant of the i -th precursor group

$k_e(t)$ Effective multiplication factor

$\ell(t)$ Prompt neutron lifetime

Introducing the variables:

$$\rho(t) = \frac{k_e(t)-1}{k_e(t)} \quad \text{Reactivity}$$

$$\Lambda(t) = \frac{\ell(t)}{k_e(t)} \quad \text{Generation time of prompt neutrons}$$

in (1) and (2), the kinetics equations become:

$$\frac{dP}{dt} = \frac{\rho(t)-\beta}{\Lambda(t)} P(t) + \sum_i \lambda_i C_i(t)$$

$$\frac{dC_i}{dt} + \lambda_i C_i(t) = \frac{\beta_i}{\Lambda(t)} P(t)$$

This model assumes that the dynamic behaviour of the reactor is independent of the space variables, a hypothesis which has been experimentally verified in numerous cases. Furthermore, on the other hand, the prompt neutron lifetime $\ell(t)$ is practically independent of time and is thus constant for a given reactor: $\ell(t) = \text{constant}$. During normal operation, the effective multiplication factor k_e is very close to unity and the prompt neutron lifetime is thus practically equal to the generation time $\ell \cong \Lambda$, i.e. $\Lambda(t)$ can also be considered to be a constant.

Now we consider a reactor in an initially critical state ($\rho = 0$). At time $t = 0$, the reactivity increases stepwise (Heaviside’s unit function) to a value of ρ and this value stays constant:



Applying the Laplace transformation to solve the above equation system gives the following characteristic equation:

$$\rho = \Lambda \omega + \sum_i \frac{\beta_i \omega}{\omega + \lambda_i} \quad i = 1 \text{ to } 6$$

The time response function of the reactor becomes:

$$\frac{P(t)}{P(0)} = \sum_j A_j \cdot \exp(\omega_j \cdot t) \quad j = 1 \text{ to } 7$$

where ω_j are the roots of the characteristic equation. The amplitude factor A_j is:

$$A_j = \frac{\Lambda + \sum_i \frac{\beta_i}{\omega_j + \lambda_i}}{\Lambda + \sum_i \frac{\lambda_i \cdot \beta_i}{(\omega_j + \lambda_i)^2}}$$

As an example, consider a reactor fuelled with ^{235}U having a generation time of $\Lambda = 10^{-3}$ s, to which a reactivity step of $\rho = +200$ pcm (+0.002) is applied. The time behaviour of the reactor:

$$\frac{P(t)}{P(0)} = \sum_{j=1}^7 A_j \cdot \exp(\omega_j \cdot t)$$

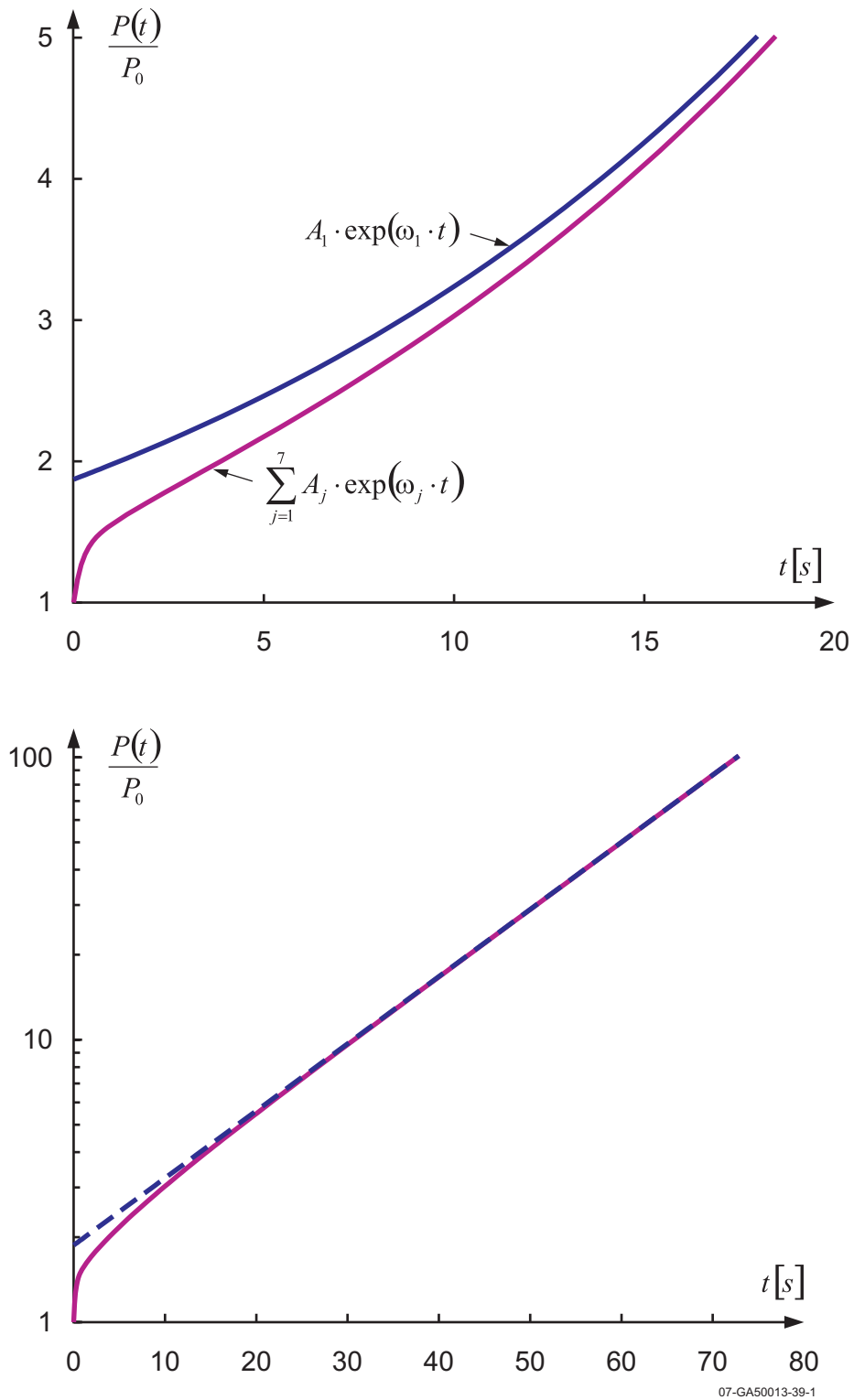
is determined by the following parameters.^a

ω_j	A_j	$1/\omega_1$
$\omega_1 = +0.0547615 \text{ s}^{-1}$	$A_1 = + 1.87251$	18.26 s
$\omega_2 = -0.0132356 \text{ s}^{-1}$	$A_2 = - 3.78731 \cdot 10^{-2}$	
$\omega_3 = -0.05183285 \text{ s}^{-1}$	$A_3 = - 2.54170 \cdot 10^{-1}$	
$\omega_4 = -0.1698684 \text{ s}^{-1}$	$A_4 = - 1.30661 \cdot 10^{-1}$	
$\omega_5 = -0.9527436 \text{ s}^{-1}$	$A_5 = - 7.60970 \cdot 10^{-2}$	
$\omega_6 = -2.708916 \text{ s}^{-1}$	$A_6 = - 6.98367 \cdot 10^{-2}$	
$\omega_7 = -5.265065 \text{ s}^{-1}$	$A_7 = - 3.03872 \cdot 10^{-1}$	

^a The kinetics parameters used to calculate these factors were determined with the code BOXER based on the JEF-1 library.

Figure 1.9 contains two plots of the corresponding function for two different time scales.

Figure 1.9. Time behaviour of the example reactor for two different time scales



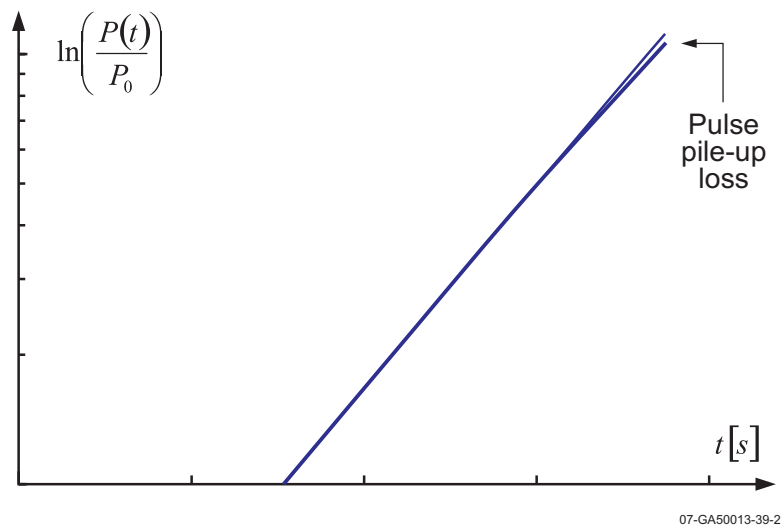
Only the first term $A_1 \cdot \exp(\omega_1 \cdot t)$ increases, all other terms die out. After 28 seconds, the difference between the exact solution and the first term $A_1 \cdot \exp(\omega_1 \cdot t)$ is 1% and decreases to about 0.1% after 53 seconds. Therefore, we can consider that the reactor power rises with a stable period of $\omega_1 = 1/\omega_1 = 18.26$ sec.

Example of measurements in CROCUS

The registration of the neutron flux as a function of time is needed in order to achieve an evaluation of the stable period of the reactor. This is done by using a multi-channel scaler (MCS) which stores the pulses issued from a fission chamber. The used MCS is a NICOLET type 370 with 2 000 channels. The dwell time can be adjusted for each experiment. The plot of the log of the channel content as a function of time shows a linear behaviour like the one represented in Figure 1.10. The slope ω_1 of this function is the inverse of the reactor period. The MCS is connected to a computer for storage and treatment of the data.

The CROCUS reactor is equipped with two CFUD21 fission chambers located in the radial reflector. Each chamber has its inner surface coated with a 93% ^{235}U enriched deposit. The associated measurement channels are of type “Multibloc” from Merlin & Gerin. These channels have a band pass of 10 MHz but the effective band pass is lower, limited for example by the charge collection time in the chamber. The pulse duration given in the specifications for the fission chambers is 250 ns. At very high pulse rates, a pile-up effect can affect the ratio between neutron flux and count rate as shown in Figure 1.10. It is important to verify this point before any measurement. There is no significant pile-up effect in CROCUS below 40 W reactor power.

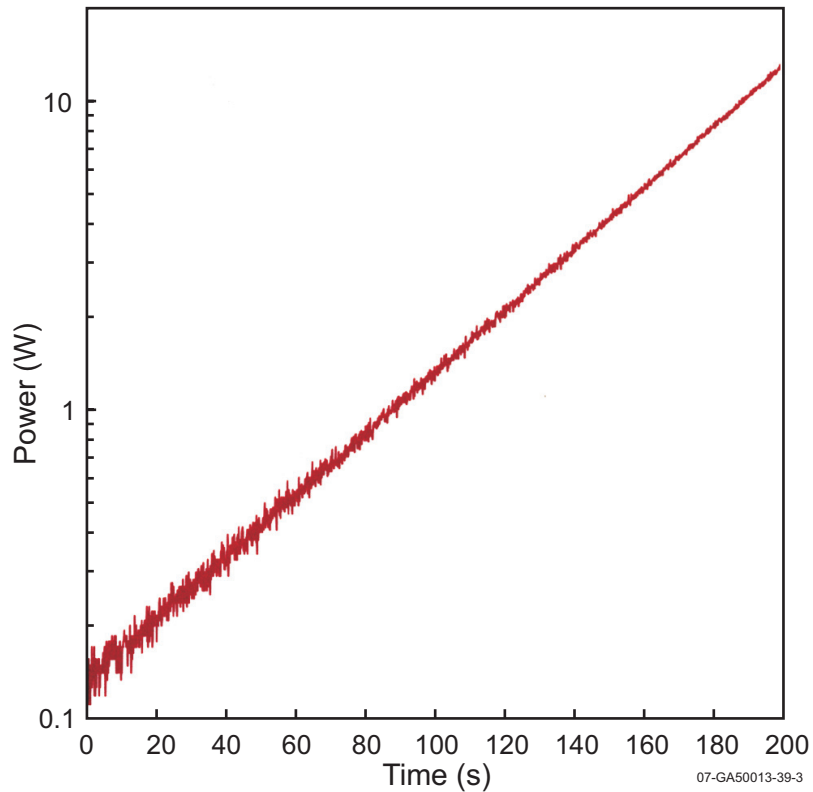
Figure 1.10. Pile-up effect affecting the ratio between neutron flux and count rate



After a reactivity step, a waiting time is needed to allow the vanishing of transients before storing the time evolution of the neutron flux. The needed waiting time has to be evaluated by using the previous equations before each measurement. In the present measurements, the waiting time was fixed by the condition that the error must be smaller than 0.1 % between the exact solution and the value of the first term $A_1 \cdot \exp(\omega_1 \cdot t)$. Finally, to obtain enough data for good statistics, the total measurement time is chosen so that the power variation reaches two decades. In CROCUS, the measurement is made between a power of about 0.1 W and 10 W. The measured pulse rate is about $7030 \text{ s}^{-1} \text{ W}^{-1}$.

Figure 1.11 shows the plotted results for a typical experiment. It should be noted that the position $t = 0$ of the time axis is an arbitrary point at the beginning of the measurement, ~30-40 sec after the reactivity jump (see discussion above).

Figure 1.11. Power as a function of time in the experiment



The function has the form:

$$\ln\left(\frac{P(t)}{P(0)}\right) = \omega_1 \cdot t + b$$

($T_1 = \frac{1}{\omega_1}$ is the stable reactor period)

By applying a linear regression analysis, the ω_1 term can be determined with a good accuracy. For the CROCUS experiments, the relative uncertainty for the ω_1 determination was max. $\pm 0.25\%$ (between ± 0.18 and $\pm 0.25\%$), with a probability of 95% that the true value is included within these margins. The corresponding uncertainty for a 1σ standard deviation is 0.2%.

Results of measurements of the inverse reactor period with variation of the water level (configuration with 172 metallic U rods)

The following Table 1.5 shows the inverse reactor periods measured at four different water levels.

Table 1.5. Measured inverse periods ω for the four different water levels in the CROCUS reactor

Case number ---	Case name ---	Water level [cm]	Inverse period ω [sec ⁻¹]
1	H ₁ = H _{crit}	96.51	0.0
2	H ₂	98.51	1.3422E-2
3	H ₃	99.00	1.8180E-2
4	H ₄	99.51	2.3392E-2

Results of measurements withdrawing an absorber rod from the centre of the configuration (with 176 metallic U rods)

In Table 1.6 are shown the inverse reactor periods measured after withdrawing each of the two absorber rods, starting from a critical situation with the absorber rod inserted.

Table 1.6. Inverse periods ω measured after withdrawing an absorber rod from the CROCUS reactor

Case number	Absorber material	Case name	Critical water level [cm]	Inverse period ω [sec ⁻¹]
5	Soluble boron	Boron	96.92	1.2856E-2
6	Erbium	Erbium	98.63	3.2976E-2

1.6.3 Material data

For the kinetics measurements, the material data are the same as for the critical configurations. They are shown in Tables 1.1-1.3.

1.6.4 Temperature data

The temperature of all materials is 20.00±0.02°C.

1.6.5 Additional information relevant to kinetics measurements

No additional information has to be given.

1.7 Description of reaction rate distribution measurements

Reaction rate distribution measurements were not performed.

1.8 Description of power distribution measurements

Power distribution measurements were not performed.

1.9 Description of isotopic measurements

Isotopic measurements were not performed.

1.10 Description of other miscellaneous types of measurements

Other types of measurements were not performed.

Chapter 2

EVALUATION OF EXPERIMENTAL DATA

2.1 Evaluation of critical and/or subcritical configuration data

2.1.1 Inaccuracies for the fuel densities

The fuel densities themselves were not measured directly but calculated with the fuel mass in the fuel rods and the volume occupied by the fuel. The inaccuracies were obtained on the basis of those for the volume and mass of the fuel rods, according to the following relation:

$$d = m / v$$

where d is the density, m the fuel mass in a rod and v the volume occupied by the fuel in the fuel rod.

Because the inaccuracies for the mass and for the volume are independent from each other, the inaccuracy for the density is given by:

$$\Delta d^2 = \left(\frac{\Delta m}{v}\right)^2 + \left(\frac{m\Delta v}{v^2}\right)^2$$

$$\Delta d = d \sqrt{\left(\frac{\Delta m}{m}\right)^2 + \left(\frac{\Delta v}{v}\right)^2}$$

$$\text{with: } \Delta v = v \sqrt{\left(2\frac{\Delta r}{r}\right)^2 + \left(\frac{\Delta H}{H}\right)^2}$$

where r is the radius of the fuel pellet and H is the height of the fuel column.

The results are shown on the last line of Table 1.2.

2.1.2 About the content of ^{234}U

No experimental data are available concerning the content of ^{234}U . The abundance of ^{234}U in natural uranium is 0.0055 at.% and that of ^{235}U is 0.72 at.% [4]. Some tests have been done with the BOXER code where the content of ^{234}U is calculated proportionally to that for ^{235}U ; at the same time the content of ^{238}U is reduced by the same amount (Table 2.1).

The two water levels H_1 and H_4 were calculated (with 15 energy groups in BOXER), each of them without and with taking the ^{234}U density into account (the total mass of uranium in the fuel is kept constant). The results of the calculated multiplication factors and the corresponding reactivity values are given in Table 2.2.

Table 2.1. Content [at.%] of the three uranium isotopes ^{234}U , ^{235}U and ^{238}U as a function of the ^{235}U enrichment

^{235}U enrichment	^{234}U	^{235}U	^{238}U
Natural	0.0055	0.7200	99.2745
1.8060 wt. %	0.0140	1.8287	98.1573
0.9470 wt. %	0.0073	0.9590	99.0337

Table 2.2. Multiplication factors and calculated reactivity values for the cases H_1 and H_4 with and without taking the ^{234}U density into account

^{234}U density	$k_{\text{eff}}(H_1)$	$k_{\text{eff}}(H_4)$	$\rho_{\text{calc}}(H_4)$ [pcm]
0.0	1.0004744	1.0017719	129.46
As Table 2.1	0.9993712	1.0006655	129.43

With ^{234}U taken into account, the multiplication factor of CROCUS decreases by ~ 110.5 pcm, but the calculated reactivity is almost not affected: it decreases by 0.03 pcm only. The kinetics parameters β (fraction of delayed neutrons) and Λ (generation time) were also obtained from both calculations for the configuration H_1 which allows determining the “kinetics” reactivity of the configuration H_4 on the basis of the measured inverse period for H_4 ($\omega(H_4) = 2.3392\text{E-}2 \text{ s}^{-1}$, Table 1.5). The results are shown in Table 2.3.

Table 2.3. “Kinetics” parameters and “kinetics” reactivity of the configuration H_4 calculated with and without taking the ^{234}U content into account

^{234}U density	β_{eff} [E-3]	Λ [E-5 s]	$\rho_{\text{kin}}(H_4)$ [pcm]
0.0	7.8252	6.1361	131.22
As Table 2.1	7.8209	6.1323	131.14

The “kinetics” reactivity of the configuration H_4 is only very little affected by the ^{234}U content: it decreases by 0.08 pcm. In such conditions, it is allowed to neglect the ^{234}U content for the present exercise.

2.1.3 Inaccuracies of the non-fuel materials

Some tests were done on the geometrical dimensions of Al grids and Cd plates; the geometrical variations considered correspond to density variations of $\sim 2\%$ for Al grids and $\sim 10\%$ for the Cd plates. The results show that the influence of these data on the reactivity is negligible (see Section 2.1.4, Table 2.6). It can be assumed that the densities given for Al and Cd are more accurate than that indicated by these values. As a consequence, corresponding inaccuracies would not provoke an error on the reactivity larger than ~ 0.01 pcm, which is negligible.

Another difficulty comes from possible impurities included in the different materials. No analysis has been done on this aspect. However, these impurities act on the multiplication factor of both the critical and the supercritical configurations in the same way; it can therefore be assumed that their influence on the (small) reactivity effects studied, which represent differences between two multiplication factors very close to each other, is negligible.

The position setting of the overflow plate is displayed with an accuracy of ± 0.1 mm. The reproducibility of the plate position is thus not better than ± 0.05 mm. An ultrasonic system allows measurement of the water level and displays it with an absolute precision of ± 0.1 mm. This is verified and calibrated once each year by absolute measurements. After setting a given overflow plate position, a fine observation of the ultrasonic signal shows that the water level is permanently fluctuating within a ± 0.1 mm band. The water level reactivity coefficient is not larger than 47 pcm/cm, i.e. the water level fluctuations introduce an error of ± 0.47 pcm on the reactivity of the configuration being measured. For the four measurements at the different water levels (Cases H₁, H₂, H₃ and H₄), the maximum uncertainty is therefore ± 0.47 pcm in each case. A conservative estimate of the uncertainty of the reactivity of the supercritical Cases H₂, H₃ and H₄ against the critical configuration H₁ can thus be assumed to be two times (± 0.47 pcm) = ± 0.94 pcm.

For the measurements with absorber rods, an additional source of uncertainty comes from the possible displacement of 2-3 mm of the lower end of the absorber rod in the bottom grid. In the case of the erbium rod, still another source of inaccuracy comes from the distribution of the pellets within the rod due to a light lack of uniformity of the pellets. The repetition of the same measurements has shown that the reactivity, after withdrawing the absorber rods, may vary by about ± 2.3 pcm, corresponding to a variation in the difference of the water levels of about ± 0.5 mm.

The water temperature is regulated through a heat exchanger connected to a cold water source. The moderator temperature is maintained at 20.00 ± 0.02 °C. The temperature coefficient is about -5 pcm/°C. This contributes to a reactivity uncertainty of ± 0.1 pcm.

2.1.4 Effect of the configuration data inaccuracies on the reactivity

The effect of inaccuracies was evaluated with 2-D BOXER calculations in 15 energy groups for both configurations H₁ = H_{crit} (water level at 96.51 cm) and H₄ (water level at 99.51 cm). Without any perturbation (i.e. on the basis of the nominal data), the reference results are as following:

$$k_{\text{eff}}(\text{H}_1) = 1.0004744, k_{\text{eff}}(\text{H}_4) = 1.0017719$$

Therefore:

$$\rho(\text{H}_4) = 10^5 [1/k_{\text{eff}}(\text{H}_1) - 1/k_{\text{eff}}(\text{H}_4)] = 129.46 \text{ pcm}$$

Results for effects of variations of the fuel rod data are given in Table 2.4. For the calculations, the increments shown as “variations” in Table 2.4 were added to the nominal data given in Table 1.2.

Table 2.4. Effects of the inaccuracies of the fuel rod data on the reactivity difference between configurations H₁ and H₄

Parameter	Unit	Variation	$k_{\text{eff}}(\text{H}_1)$	$k_{\text{eff}}(\text{H}_4)$	ρ [pcm]	$\Delta\rho$ [pcm]
Clad thickness	mm	+0.05	1.0001964	1.0014898	129.12	-0.34
Outer clad diameter	mm	+0.1	1.0006872	1.0019879	129.72	+0.26
Fuel diam. UO ₂ /U _{metal}	mm	+0.017/+0.02	1.0008912	1.0021876	129.24	-0.22
²³⁵ U enrichment	wt. %	+0.0007	1.0006235	1.0019212	129.44	-0.02
Square pitch	mm	+0.002	1.0004636	1.0017611	129.46	+0.00
Fuel density UO ₂ /U _{metal}	g/cm ³	+0.034/+0.044	1.0009149	1.0022113	129.24	-0.22

The effects of the inaccuracies of the axial data (see Table 1.1) were evaluated through axial calculations of the central part of CROCUS (i.e. along the UO₂ zone), followed by a calculation of the extrapolated height H_{extr} (based on a cosine fit of the axial power density distribution; see Section 3.1) and the determination of the axial buckling B_z^2 according to:

$$B_z^2 = \left(\frac{\pi}{H_{extr}} \right)^2$$

The effects of these inaccuracies on the reactivity are very small and therefore the 2-D configurations were not calculated with BOXER, but their reactivity was evaluated according to the following scheme: In BOXER, the multiplication factor k_{eff} is calculated as:

$$k_{eff} = \frac{P}{A + L_r + L_z}$$

where P is the production; the flux normalisation is such that $P = 1.0$. A is the absorption, L_r the radial leakage and L_z the axial leakage.

The reactivity of the configuration H_4 is given by:

$$\rho = \frac{1}{k_{eff}(H_1)} - \frac{1}{k_{eff}(H_4)} = (A + L_r + L_z)_1 - (A + L_r + L_z)_4$$

A perturbation of a certain item of configuration data provokes a variation of the multiplication factors of the critical configuration H_1 as well as of the supercritical one H_4 . The results of the perturbed case are noted with a tilde (\sim). The resulting difference in the reactivity produced by the perturbation is therefore:

$$\Delta\rho = \tilde{\rho} - \rho = (\tilde{A} + \tilde{L}_r + \tilde{L}_z)_1 - (\tilde{A} + \tilde{L}_r + \tilde{L}_z)_4 - (A + L_r + L_z)_1 + (A + L_r + L_z)_4$$

The 2-D calculation is done for a horizontal plane at about the middle height of the core, so that the axial perturbation affects neither the absorption nor the radial leakage of the 2-D calculation. Therefore, it can be assumed that:

$$\tilde{A} = A \text{ and } \tilde{L}_r = L_r$$

so that:

$$\Delta\rho = (\tilde{L}_z - L_z)_1 - (\tilde{L}_z - L_z)_4$$

but $L_z = M^2 B_z^2$ and M^2 is the migration area.

For the same reason as for A and L_r , M^2 is not affected by an axial perturbation. One then has:

$$\Delta\rho = M_1^2 (\tilde{B}_z^2 - B_z^2)_1 - M_4^2 (\tilde{B}_z^2 - B_z^2)_4$$

The values of M_1^2 , B_{z1}^2 , M_4^2 and B_{z4}^2 are taken from calculations of the unperturbed configurations (i.e. based on nominal data). They are given in Table 2.5.

Table 2.5. Values of the bucklings and migration area for unperturbed configurations H₁ and H₄

Configuration	B_z^2 [cm ⁻²]	M^2 [cm ²]
H ₁	$9.0103 \cdot 10^{-4}$	34.101
H ₄	$8.6076 \cdot 10^{-4}$	34.091

The inaccuracies of the axial data given in Table 1.1 were taken into account by considering perturbations of the nominal data. The resulting variations of the reactivity are shown in Table 2.6.

Table 2.6. Effect of the inaccuracies of the axial data on the reactivity between configurations H₁ and H₄

Parameter	Variation [mm]	H ₁		H ₄		$\Delta\rho$ [pcm]
		H _{extr} [cm]	B_z^2 [cm ⁻²]	H _{extr} [cm]	B_z^2 [cm ⁻²]	
Base plate	+0.1	104.66	$9.0103 \cdot 10^{-4}$	107.08	$8.6076 \cdot 10^{-4}$	0
Lower grid a	+0.1	104.66	$9.0103 \cdot 10^{-4}$	107.08	$8.6076 \cdot 10^{-4}$	0
Lower Cd plate	+0.05	104.66	$9.0103 \cdot 10^{-4}$	107.08	$8.6076 \cdot 10^{-4}$	0
Lower grid b	+0.1	104.67	$9.0086 \cdot 10^{-4}$	107.09	$8.6060 \cdot 10^{-4}$	-0.03
Upper grid a	+0.1	104.66	$9.0103 \cdot 10^{-4}$	107.08	$8.6076 \cdot 10^{-4}$	0
Upper Cd plate	+0.05	104.66	$9.0103 \cdot 10^{-4}$	107.08	$8.6076 \cdot 10^{-4}$	0
Upper grid b	+0.1	104.66	$9.0103 \cdot 10^{-4}$	107.08	$8.6076 \cdot 10^{-4}$	0
Upper rod parts	+0.5	104.66	$9.0103 \cdot 10^{-4}$	107.08	$8.6076 \cdot 10^{-4}$	0

As can be seen from Table 2.6, inaccuracies of the axial data have quite a negligible influence on the reactivity.

In the two absorber rod cases, the axial bucklings for the critical configurations (i.e. the configurations with the absorber rod inserted) are not given, but they must be determined by each calculation method. The resulting multiplication factor is therefore equal to 1.0 for each of the two cases. After withdrawing the absorber rod, the multiplication factor of the supercritical configuration has to be determined with the same value for the axial buckling. This calculation was done with BOXER with 15 energy groups. First, the reference values for the unperturbed configurations (nominal data) were obtained (see Table 2.7).

Table 2.7. BOXER results (15 energy groups) for the reactivity of CROCUS after withdrawing the absorber rod

Poison rod	Configuration	B_z^2 [cm ⁻²]	k_{eff}	ρ [pcm]
Boron	H ₅	$9.19045 \cdot 10^{-4}$	1.0008350	83.43
Erbium	H ₆	$8.94552 \cdot 10^{-4}$	1.0016418	163.91

The inaccuracies of the absorber rod data as given in Table 1.3 were taken as perturbations of the nominal data. The resulting variations of the reactivity are shown in Table 2.8. In this table, the axial bucklings B_z^2 are the critical ones (i.e. for $k_{eff} = 1.0$) with the absorber rod inserted and the corresponding perturbation being taken into account, while \tilde{k}_{eff} is the multiplication factor after withdrawing the absorber rod but with the same axial buckling.

Table 2.8. Effect of the inaccuracies of the absorber rod data on the reactivity after withdrawing the absorber rod

Parameter	Poison	B_z^2 [cm ⁻²]	\tilde{k}_{eff}	$\tilde{\rho}$ [pcm]	$\Delta\rho$ [pcm]
Al clad radius in/out: +0.05 mm	Boron	$9.18309 \cdot 10^{-4}$	1.0008592	85.85	+2.42
	Erbium	$8.94400 \cdot 10^{-4}$	1.0016468	164.41	+0.50
Al clad thickness: +0.05 mm	Boron	$9.18956 \cdot 10^{-4}$	1.0008379	83.72	+0.29
	Erbium	$8.94399 \cdot 10^{-4}$	1.0016469	164.42	+0.51
Boron density: +0.1%	Boron	$9.19023 \cdot 10^{-4}$	1.0008357	83.50	+0.07
Er pellet density: +1.0%	Erbium	$8.94234 \cdot 10^{-4}$	1.0016523	164.96	+1.05
Er pellet diameter: +0.2%	Erbium	$8.94438 \cdot 10^{-4}$	1.0016459	164.32	+0.41

2.1.5 Summary of the effects of the configuration data inaccuracies on the reactivity

All the perturbations studied above are independent from each other. Their effects can therefore be summed using the statistical formula:

$$\Delta\rho = \pm \sqrt{\sum_i (\Delta\rho_i)^2}$$

For configuration H₄, the effects to be considered are given in Tables 2.4 and 2.6. The result is:

$$\Delta\rho(H_4) = \pm 0.53 \text{ pcm}$$

For both configurations H₂ and H₃, it is assumed that the ratio $\Delta\rho/\rho$ is a constant. Therefore:

$$\Delta\rho(H_i) = \rho_{\text{mean}}(H_i) \cdot \Delta\rho(H_4) / \rho_{\text{mean}}(H_4)$$

Taking as ρ_{mean} the mean results given in Table 4.3, one finds:

$$\Delta\rho(H_2) = \pm 0.36 \text{ pcm}, \Delta\rho(H_3) = \pm 0.45 \text{ pcm}$$

For both cases with absorber rods, the results from Table 2.8 have to be considered further. One has:

$$\Delta\rho^2(\text{abs.rod}) = [\rho_{\text{mean}}(\text{abs.rod}) \cdot \Delta\rho(H_4) / \rho_{\text{mean}}(H_4)]^2 + \sum_i \Delta\rho_i^2 \text{ (Table 2.8)}$$

For boron, one finally obtains:

$$\Delta\rho(H_5) = \pm 2.46 \text{ pcm}$$

For erbium, one finally obtains:

$$\Delta\rho(H_6) = \pm 1.50 \text{ pcm}$$

Conclusion

The effects of all material and geometrical data uncertainties on the reactivity between two configurations close to each other are small enough so that the described CROCUS configuration can be used as a reference for checking the kinetics parameters calculated for the studied configurations. This method can be used because the same fuel rods at the same locations are used for both the supercritical configurations and the corresponding critical configuration.

2.2 Evaluation of buckling and extrapolation length data

Buckling and extrapolation length measurements were not performed.

2.3 Evaluation of spectral characteristics data

Spectral characteristics measurements were not performed.

2.4 Evaluation of reactivity effects data

Reactivity effects measurements were performed, but have not yet been evaluated.

2.5 Evaluation of reactivity coefficient data

Reactivity coefficient measurements were not performed.

2.6 Evaluation of kinetics measurement data

By repeating the same experiment many times, the maximal difference in the measured inverse reactor period ω was found to be $\pm 1.4\%$ (Section 1.6.2). This uncertainty includes mostly three different terms:

- effect of the transients after the reactivity jump (terms of higher order);
- pile-up effect;
- linear regression analysis.

The other effects as evaluated in Tables 2.4, 2.6 and 2.8 are not included. According to the largest differences in ω obtained by different measurements of the same configuration, it is proposed that the global experimental uncertainty of the CROCUS period measurements be considered as being $\pm 0.7\%$ (relative, 1σ). Within this uncertainty range, these measurements can be used as reference results for the proposed benchmark exercise on kinetics parameters.

2.7 Evaluation of reaction rate distributions

Reaction-rate distribution measurements were not performed.

2.8 Evaluation of power distribution data

Power distribution measurements were not performed.

2.9 Evaluation of isotopic measurements

Isotopic measurements were not performed.

2.10 Evaluation of other miscellaneous types of measurements

Other miscellaneous types of measurements were not performed.

Chapter 3

BENCHMARK SPECIFICATIONS

The present benchmark exercise is devoted to check the methods and basic kinetics parameters used in the calculation of the delayed neutron fraction β_{eff} and the generation time Λ . For that, the reactivity of a supercritical reactor configuration is calculated in two different manners:

- a) By direct calculation of the critical configuration and the corresponding supercritical configuration. The comparison of the two multiplication factors allows determining the calculated reactivity ρ_{calc} .
- b) By using the kinetics parameters from the calculation of the critical configuration and the measured inverse reactor period. The resulting reactivity is called the “kinetics” reactivity ρ_{kin} .

3.1 Benchmark model specifications for critical and/or subcritical measurements

Although criticality has not been fully evaluated, model specifications are given here as the basis for the evaluation of the kinetic parameters.

3.1.1 Description of the benchmark model simplifications

For a given calculation method, the calculated reactivity will be assumed to be the reference value for the “kinetics” reactivity. For measurements done at different water levels, it can be assumed that a discrepancy in the calculated multiplication factors will be the same for the critical configuration and the supercritical configurations, such that the calculated reactivity will be affected only in a negligible manner. It is therefore not necessary to tend to a very accurate calculation of the multiplication factors.

The problem is more difficult for both cases with absorber rods: it is not very easy to model the small absorber rod located between the four central fuel rods, especially in the case of the erbium rod where the cross-sections of the Er isotopes and the calculation of their resonance shielding is another difficulty. The discrepancy of the calculated k_{eff} for the critical configuration (with the absorber rod inserted) against the experimental value (i.e. $k_{\text{crit}} = 1.0$) would give information about the quality of the calculation of the absorber rod. But this is not the purpose of the present benchmark; it is the reason why it is proposed that each calculation method determines its own critical water level for the cases with absorber rod inserted. The reactivity of the absorber rod is then obtained by the calculation of the same configuration (with the same water level), but after withdrawing the absorber rod. The difference between this calculated reactivity and the reactivity based on the kinetics parameters and the measured inverse reactor period will include not only the inaccuracy of the kinetics parameters but also the inaccuracy of the model of the absorber rod.

3.1.2 Dimensions

Variation of the water level

The critical configuration (Case 1) is based on the fuel cell distribution displayed in Figure 1.4, which counts 172 metallic U rods. The criticality is reached for a water level of $H_1 = H_{\text{crit}} = 96.51$ cm. The configuration has an eight-fold symmetry. It is therefore sufficient to model only one quarter of it with reflective boundary conditions on two sides. The water reflector around the reactor core can be assumed as infinite. If the reflector thickness is reduced to ~20 cm, the effect on the reactivity between two close configurations is negligible.

Using Figure 1.3 and the data in Sections 1.1.2 and 1.1.3, a 3-D model of the CROCUS reactor can be established. As the goal of the present exercise is to compare calculated and “kinetics” reactivity values, it is suggested to limit the axial description of the configuration to the top surface of the upper Cd layer. The very small underestimation of the calculated multiplication factors due to this limitation will affect neither the calculated reactivity nor the kinetics parameters obtained for the critical configuration.

Figure 3.1 shows a 90° sector for a 3-D model together with the axial dimensions. The geometry of the UO_2 and the U_{metal} rods is illustrated in Figure 3.2.

To allow two-dimensional calculations of the configurations, axial bucklings are also given as part of the configuration description (see Table 3.5). These bucklings were not measured, but determined on the basis of axial calculations in the inner region of the reactor (oxide fuel). For these calculations, all the different axial regions of the core as shown in Figure 1.3 (for the UO_2 zone only) were accurately described. The results of the following 1-D axial calculation are the axial distribution of the flux and power density along the UO_2 fuel column. Afterwards, the extrapolated height and the corresponding axial buckling were determined based on the cosine fit of the axial power density. An inaccuracy of the buckling values affects directly the calculated multiplication factors k_{eff} of the considered configuration, but as it affects in the same manner the critical configuration H_1 and the supercritical ones, it will have practically no influence on the calculated reactivity effects. The kinetics parameters will also not be affected.

Configurations with an absorber rod

For the configurations with an absorber rod, the distribution of the fuel rods as shown in Figure 3.3 with 176 metallic U rods is to be modelled. The small absorber rod is located at the very centre of the configuration between the four central UO_2 rods. This configuration has only a two-fold symmetry according to the first diagonal. The axial distribution of materials as deduced from Figure 1.3 is the same as shown in Figure 3.1, with the different rod types illustrated in Figure 3.2.

The critical water level (for 3-D calculations) should not be used; the bucklings (for 2-D calculations) for the critical cases are not given. Instead, the critical water height or the axial bucklings should be determined by each calculation method to obtain criticality by adjusting the water height, or by a buckling search for k_{eff} equal to 1.0, with the absorber rod inserted. Afterwards, the absorber rod is removed and the supercritical configuration has to be calculated for the same water level or with the same buckling value. (Remember: removing the absorber rod does not affect the water level.)

Notice: For critical cases with an absorber rod inserted, it is possible to calculate the 3-D configurations with the water level given in Table 3.6, or to determine a buckling value for 2-D models. This option is not proposed here because it is fairly difficult to model the configuration with an absorbing rod

inserted between the four central fuel rods, especially in the case of erbium absorber where the calculation of the resonance shielding of the Er isotopes is still another problem. The described method was proposed using the assumption that the difference of two multiplication factors fairly close to each other (or the reactivity difference between two configurations close to each other) is not greatly affected by inaccuracies in the multiplication factors themselves, because both compared multiplication factors are calculated using the same approximations. In that way, the problem of comparing eventually different multiplication factors from two different calculation methods can be avoided. (Remember: the goal of the exercise is not to compare multiplication factors but kinetics parameters.)

Figure 3.1. 3-D model for the measurements with variation of the water level

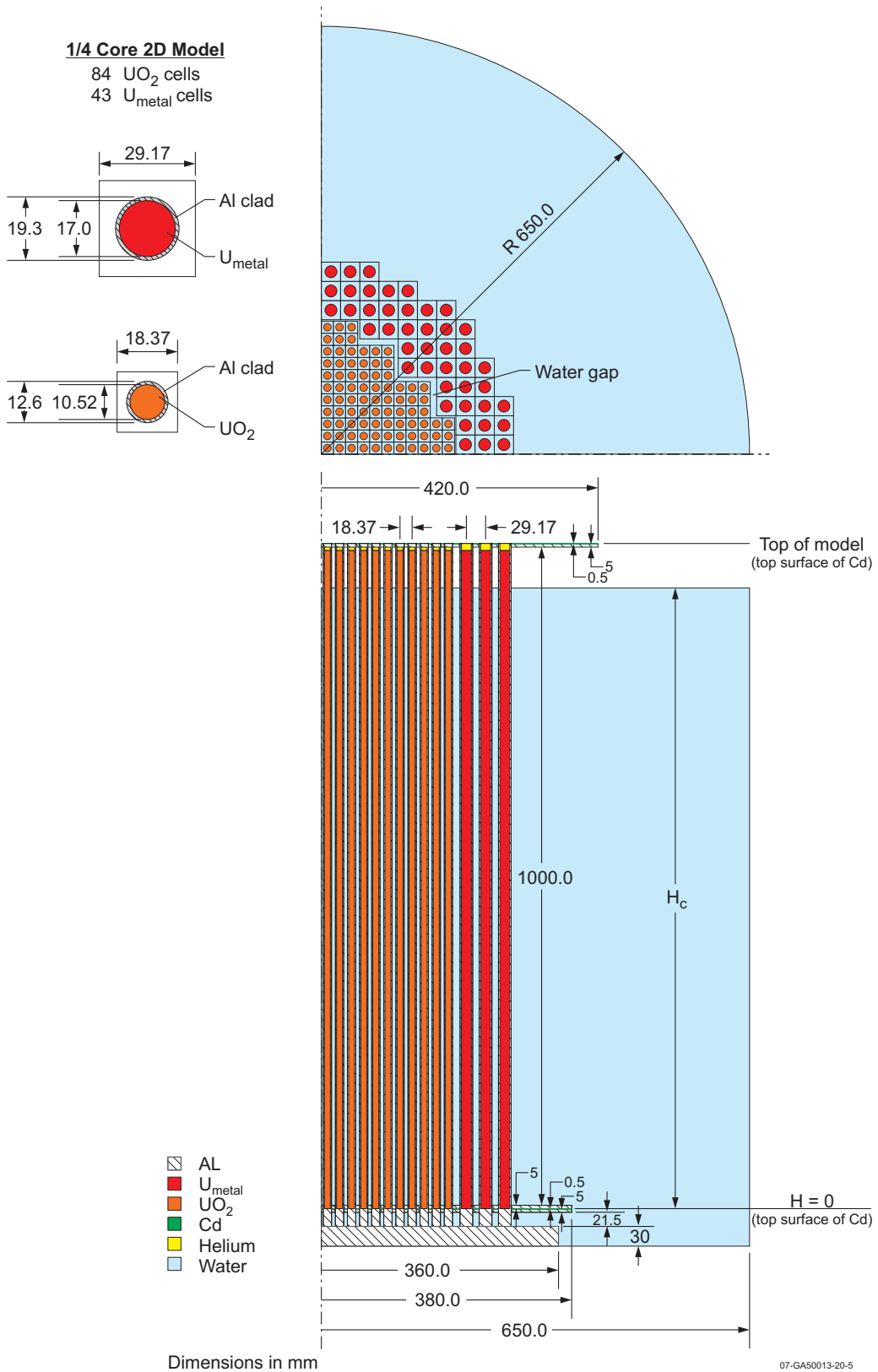
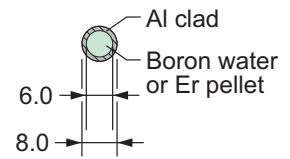
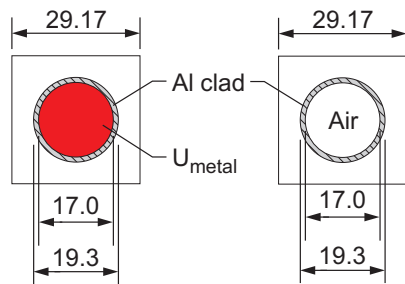
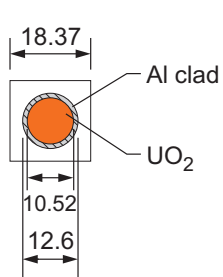
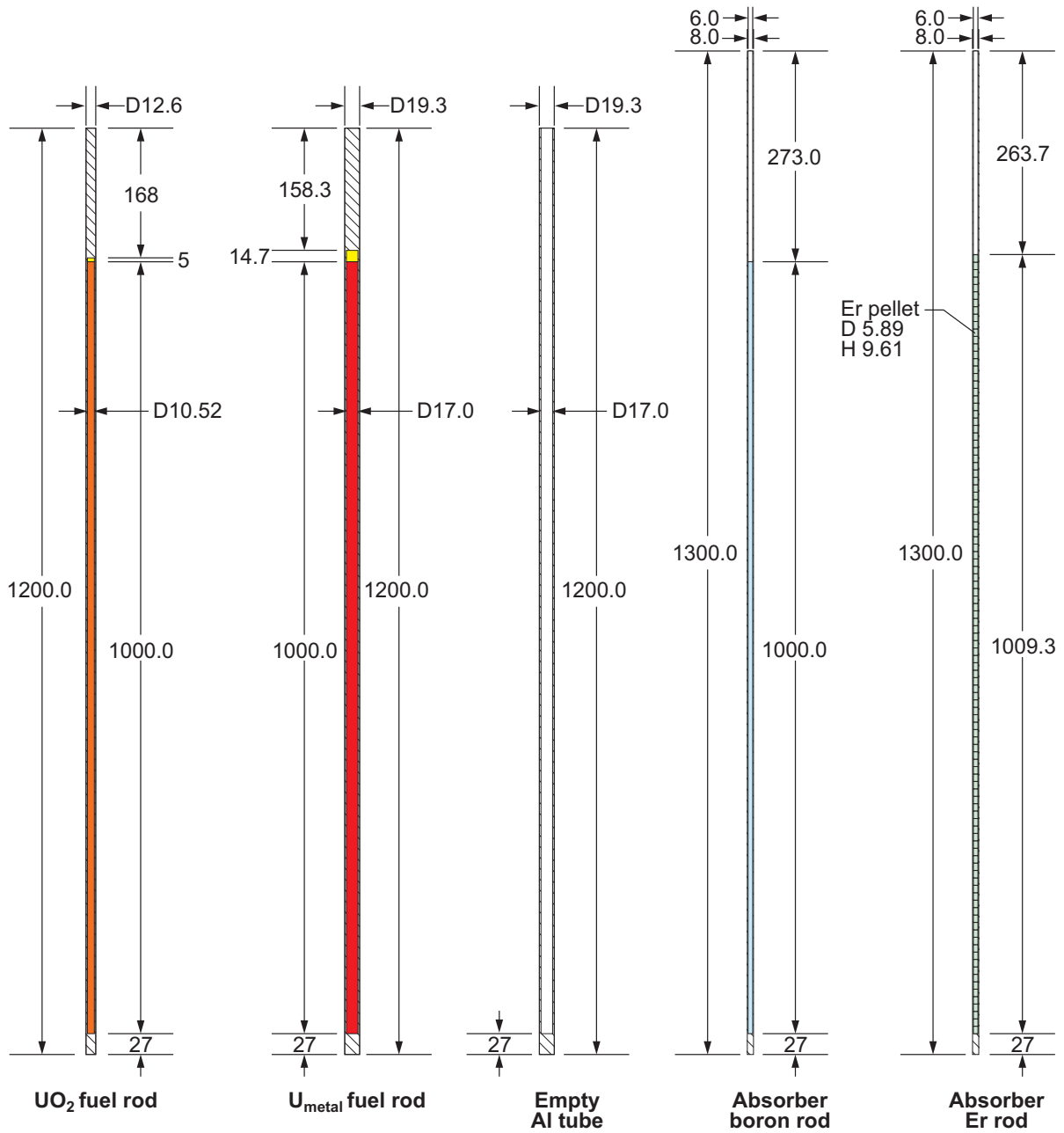
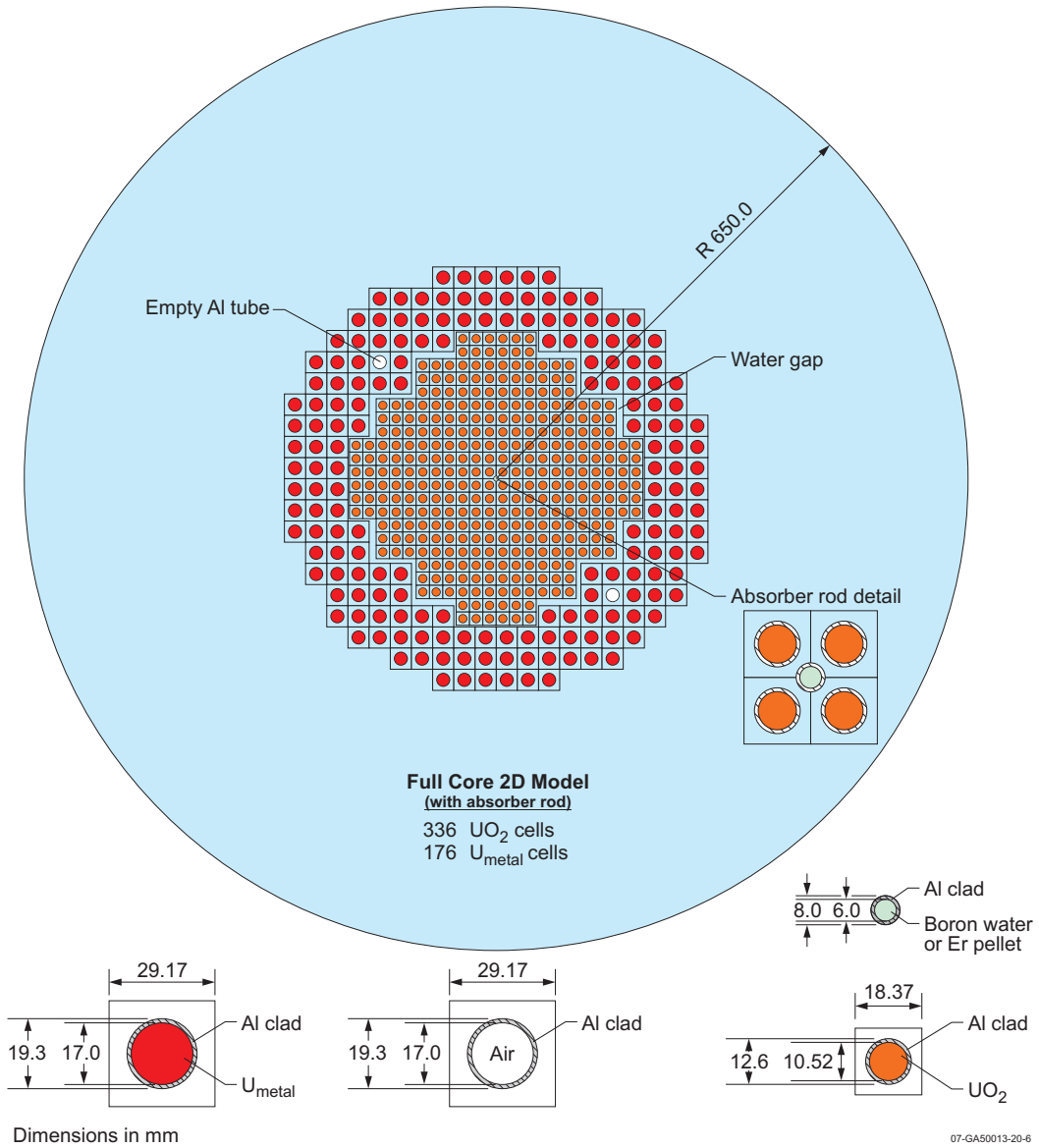


Figure 3.2. Geometry of the different rod types in CROCUS



Dimensions in mm
07-GA50013-20-4

Figure 3.3. Core cross-section for the measurements with absorber rods



The dimensions of the different material regions appearing in the CROCUS reactor are described in Table 3.1. The reactor vessel has an inner radius of 65 cm and a wall thickness of 1.2 cm.

Table 3.1. Nominal data to be used in the computer model for the CROCUS reactor

a) Fuel rods

Parameter	Unit	UO ₂	U _{metal}
Cladding thickness	mm	0.85	0.975
External cladding diameter	mm	12.6	19.3
Fuel diameter	mm	10.52	17.0
Square pitch	mm	18.370	29.17

b) Thickness of axially partitioned structure materials

Parameter	Dimension [mm]
Base plate	30.0
Lower grid a	5.0
Lower Cd plate	0.50
Lower grid b (Lgb)	5.0
Distance between Lgb and Uga	1 000
Upper grid a (Uga)	5.0
Upper Cd plate	0.50
Upper grid b	15.0
Upper part of rods	147.5

c) Absorber rods

Parameter	Dimension [mm]
Outer diameter	8.0
Wall thickness	1.0
Er absorber: pellet diameter	5.89

3.1.3 Material data

Table 3.2 gives the atomic densities of the materials appearing in the fuel region of the CROCUS reactor. The isotopic abundances are taken from Ref. [4] while the Avogadro number comes from Ref. [3]. (The data are taken from the output of the BOXER code, Section A.8.1.)

Table 3.2. Atomic densities of the materials appearing in the fuel cells of the CROCUS reactor

Material	Nuclide	Atomic density [E+24/cm ³]	
		UO ₂	Metallic U
Fuel	¹⁶ O	4.70902E-02	0.0
	²³⁵ U	4.30565E-04	4.53160E-04
	²³⁸ U	2.31145E-02	4.68003E-02
Clad ^(a)	Al	5.00614E-02	5.17799E-02
Moderator	¹ H	6.67578E-02	
	¹⁶ O	3.33789E-02	

^(a) The gap between fuel pellet and clad is homogenised with the clad.

The atomic densities of the non-fuel materials are listed in Table 3.3. The screws and springs may be omitted because they are located above the water level, therefore they do not affect the reactivity difference between two configurations close to each other.

Table 3.3. Atomic densities of non-fuel materials in the CROCUS reactor

Name	Material	Nuclide	Atomic density [E+24/cm ³]
Base plate Lower & upper grids	Al	Al	6.02611E-02
End plugs Cladding			
Cadmium layers	Cd	Cd	4.63334E-02
Moderator	Water	¹ H	6.67578E-02
		¹⁶ O	3.33789E-02
Filler gas (fuel rods)	Helium	⁴ He	1.64E-4
Air above water level	Air	¹⁴ N	4.14E-05
		¹⁶ O	9.07E-06

Absorber rods

As mentioned, two neutron absorber rods were inserted, one at a time, in the centre of the core. The absorber rods were clad in cylindrical aluminium tubes. The first rod was filled with water which contained 6 768 ppm natural boron. The second rod contained pellets with 3.72 g/cm³ ZrO₂ and 0.874 g/cm³ Er₂O₃ (i.e. 0.764 g/cm³ Er). The corresponding atomic densities for the materials of the absorber rods are shown in Table 3.4. The fuel rod configuration used for the measurements with absorber rods also contains two empty rods instead of the corresponding metallic U rods. For such empty rods, the Al cladding was homogenised with the moderator over the full volume of the cell.

3.1.4 Temperature of materials

The temperature of all materials of all configurations is 20°C.

3.1.5 Experimental and benchmark model k_{eff} and/or subcritical parameters

Criticality is not fully evaluated. Model specifications are only given as basis for the evaluation of kinetic parameters.

3.2 Benchmark model specifications for buckling and extrapolation-length measurements

Buckling and extrapolation-length measurements were not performed.

3.3 Benchmark model specifications for spectral characteristics measurements

Spectral characteristics measurements were not performed.

Table 3.4. Atomic densities of the absorber rods and the empty rods

Absorber rod	Region	Nuclide	Atomic density [E+24/cm ³]
Boron	Borated water	¹ H	6.67578E-02
		¹⁶ O	3.33789E-02
¹⁰ B		7.48861E-05	
¹¹ B		3.01426E-04	
	Clad	Al	6.02611E-02
Erbium	Er-Zr pellet	¹⁶ O	4.04919E-02
		Zr	1.81819E-02
		¹⁶² Er	3.85287E-06
		¹⁶⁴ Er	4.43080E-05
		¹⁶⁶ Er	9.24688E-04
		¹⁶⁷ Er	6.31595E-04
		¹⁶⁸ Er	7.37549E-04
	¹⁷⁰ Er	4.10055E-04	
	Clad ^(a)	Al	5.75719E-02
Empty Al rod	Air	¹⁴ N	4.14E-05
		¹⁶ O	9.07E-06
	Al tube	Al	6.02611E-02
	Moderator	¹ H	6.67578E-02
¹⁶ O		3.33789E-02	

(a) The gap between Zr-Er pellets and the clad was homogenised with the clad.

3.4 Benchmark model specifications for reactivity effects measurements

Reactivity measurements were not performed.

3.5 Benchmark model specifications for reactivity coefficient measurements

Reactivity coefficient measurements were not performed.

3.6 Benchmark model specifications for kinetics measurements

3.6.1 Description of the benchmark model simplifications

Because the upper part of the fuel rods are extending above the water level and this part of the fuel length changes with variation of the water level, this exercise is more a R-Z or three-dimensional problem than a X-Y or R- θ (two-dimensional) one. It is not possible to simulate the variation of the water level via the direct change in π^2/H^2 .

In order to allow two-dimensional calculations, the axial bucklings corresponding to the different water levels have been obtained through a 1-D axial calculation of the UO₂ region of CROCUS, followed by cosine-fitting of the axial power distributions. The model used is an accurate description of all axial zones of the UO₂ fuel region of the core as given in Figure 1.3. The bucklings are given in Table 3.5.

Table 3.5. CROCUS data for the different water levels and corresponding measured inverse periods ω

Case number ---	Case name ---	Water level ^(a) [cm]	Axial buckling ^(b) [cm ⁻²]
1	H ₁ = H _{crit}	96.51	9.0900E-4
2	H ₂	98.51	8.8222E-4
3	H ₃	99.00	8.7591E-4
4	H ₄	99.51	8.6967E-4

^(a) To be used for three-dimensional or R-Z-calculations.

^(b) To be used for two-dimensional calculations (X-Y, R- θ).

The reactivity effects in the absorber rod measurements can be calculated by two-dimensional codes by searching for the critical buckling with the absorber rod inserted and using the same buckling in a second calculation without the absorber rod (i.e. water instead of the rod). With 3-D calculations, the water height has to be adjusted such that $k_{\text{eff}} = 1.0$ with the absorber rod inserted; after withdrawing the absorber rod, the calculation is repeated with the same water height.

3.6.2 Dimensions

The configuration geometry and measurement procedure are the same as described in Section 3.1.3 for the critical configurations.

3.6.3 Material data

The material data are the same as given in Section 3.1.3 for the critical configurations.

3.6.4 Temperature data

The temperature of all materials of all configurations is 20°C.

3.6.5 Experimental and benchmark model kinetics measurements

Table 3.6 contains the measured inverse reactor periods for the three supercritical configurations without absorbers and the two with absorbers together with the respective critical water level.

Table 3.6. Inverse periods ω in the CROCUS reactor

Case number	Absorber material	Case name	Critical water level [cm]	Inverse period ω [sec ⁻¹]
1	No absorber	H ₁ = H _{crit}	96.51	0.0
2	No absorber	H ₂	98.51	1.3422E-2
3	No absorber	H ₃	99.00	1.8180E-2
4	No absorber	H ₄	99.51	2.3392E-2
5	Soluble boron	Boron	96.92	1.2856E-2
6	Erbium	Erbium	98.63	3.2976E-2

3.7 Benchmark model specifications for reaction rate distribution measurements

Reaction rate distribution measurements were not performed.

3.8 Benchmark model specifications for power distribution measurements

Power distribution measurements were not performed.

3.9 Benchmark model specifications for isotopic measurements

Isotopic measurements were not performed.

3.10 Benchmark model specifications for other miscellaneous types of measurements

Other miscellaneous types of measurements were not performed.

Chapter 4

RESULTS OF SAMPLE CALCULATIONS

The benchmark was calculated by three participants: Framatome ANP, the Kurchatov Institute and the Paul Scherrer Institute (PSI), with a total of four different calculation methods. The methods are as follows: HEXNOD is a deterministic transport code, used in its 2-D version and its group constants being prepared by CASMO-4. The pointwise Monte Carlo code MCU-REA is used in two dimensions. HELIOS is a general 2-D neutron physics transport code applicable to almost every 2-D configuration. BOXER is a cell and 2-D transport code in X-Y geometry. In a first step, the eigenvalue of the critical configuration and the reactivity changes for the five supercritical cases were calculated (“calculated” reactivity). In a second step, kinetics parameters for the critical configurations were obtained from the same code and then used, together with the measured inverse reactor periods, to calculate the reactivity changes by the inhour equation (“kinetics” reactivity). Assuming that the initially calculated reactivity effects are correct, comparison of the two sets of results, i.e. “calculated” and “kinetics” reactivity changes, provides an assessment of the accuracy of the kinetics parameters.

4.1 Results of calculations of the critical or subcritical configurations

The critical configuration with a water level of $H_1 = 96.51$ cm (or with the given axial buckling of $9.0900E-4$ cm^{-2} for two-dimensional calculations) was calculated by all codes. Table 4.1 summarises the calculated multiplication factors from the different participants. The largest discrepancy against the experimental value (i.e. $k_{\text{eff}} = 1.0$) in the results for the calculation of the critical configuration is smaller than 300 pcm. This indicates that all the employed models of the CROCUS reactor are in principle correct and should be expected to yield reliable calculated results for reactivity changes of the type currently considered.

Table 4.1. Calculated multiplication factors for the critical configuration H_1

Name of code	HEXNOD	MCU	HELIOS	BOXER
Used library	ENDF/B-4	MCUDAT	ENDF/B-6	JEF-1
Calculated k_{eff}	0.99811	0.99713	1.00090	1.00094

4.2 Results of buckling and extrapolation length calculations

Buckling and extrapolation measurements were not performed.

4.3 Results of spectral characteristics calculations

Spectral characteristics measurements were not performed.

4.4 Results of reactivity effects calculations

Reactivity effects measurements were not performed.

4.5 Results of reactivity coefficient calculations

Reactivity coefficient measurements were not performed.

4.6 Results of kinetics parameter calculations

4.6.1 Calculated kinetics parameters for Case 1 ($H_1 = H_{crit}$)

In this section, the kinetics parameters calculated for the critical configuration H_1 by the different methods are compared to each other. Table 4.2(a) shows the results for the effective delayed neutron fractions β_{eff} . Fairly large differences (up to almost 10%) can be observed in the total fraction, the relative discrepancies being much larger for the six individual precursor groups.

Table 4.2(a). Comparison of the effective delayed neutron fractions [10^{-3}] for the critical configuration $H_1 = H_{crit}$

	β_{eff}	β_1	β_2	β_3	β_4	β_5	β_6
Mean	7.4737	0.2426	1.4545	1.3558	2.9683	1.1043	0.3474
HEXNOD	7.1855	0.2458	1.4461	1.3226	2.9034	1.0267	0.2409
MCU	7.533	0.2222	1.550	1.435	2.968	1.000	0.3568
HELIOS	7.2975	0.2328	1.2457	1.2143	2.8208	1.2597	0.5242
BOXER	7.8257	0.2698	1.5652	1.4414	3.1602	1.1239	0.2652

The calculated generation times Λ and the decay constants of each precursor group are shown in Table 4.2(b). The differences in Λ are of the same order of magnitude as for the effective delayed neutron fractions. For the decay constants λ , both methods HEXNOD and BOXER show a good agreement between each other. The values given by MCU are systematically lower, especially in the precursor Groups 4, 5 and 6 (the difference reaches 30% in the last two groups). The HELIOS values are larger in Groups 1 to 4 and smaller in Groups 5 and 6.

Table 4.2(b). Comparison of the generation time Λ [sec] and the decay constants λ_i [sec^{-1}] for the critical configuration $H_1 = H_{crit}$

	Λ [10^{-5} s]	λ_1 [s^{-1}]	λ_2 [s^{-1}]	λ_3 [s^{-1}]	λ_4 [s^{-1}]	λ_5 [s^{-1}]	λ_6 [s^{-1}]
Mean	5.9291	0.01291	0.03138	0.1187	0.3163	1.197	3.495
HEXNOD	5.7	0.012750	0.031780	0.11911	0.31806	1.4024	3.9238
MCU	5.961	0.0125	0.03062	0.1130	0.3051	1.067	3.084
HELIOS	5.9234	0.013627	0.031340	0.12328	0.32359	0.9058	3.0484
BOXER	6.132	0.012752	0.031782	0.11925	0.31839	1.4025	3.9258

Notice: The comparison of the values of kinetics parameters per group (β_i and λ_i) does not make much sense because these parameters depend on the list of precursors considered in each group i , which may vary from one library to the other. But of course, the macroscopic parameters β_{eff} and Λ should be consistent, no matter with which library they were calculated.

4.6.2 Calculated reactivity effects

The reactivity of the supercritical configurations was calculated through the different codes as:

$$\rho_{calc} [\text{pcm}] = 10^5 \left[\frac{1}{k_{eff}(crit)} - \frac{1}{k_{eff}(perturb)} \right]$$

where $k_{eff}(crit)$ is the calculated multiplication factor for the critical configuration $H_1 = H_{crit}$ and $k_{eff}(perturb)$ is the calculated multiplication factor taking the perturbation into account.

The experimental uncertainty is composed of four terms resulting from:

- Uncertainty of critical configuration data; see Section 2.1.5 for values corresponding to this term;
- Uncertainty of the water level; this term corresponds to ± 0.94 pcm on the reactivity for the three cases H_2 to H_4 and ± 2.3 pcm for both cases H_5 and H_6 (see Section 2.1.3);
- Uncertainty on the temperature; this corresponds to ± 0.1 pcm on the reactivity (see Section 2.1.3);
- Uncertainty on the measured inverse period of $\pm 0.7\%$ on ω (see Section 2.6). For the Case H_4 , a 10% increase on ω corresponds to an increase of 6.4% of the reactivity (see below). Therefore the uncertainty of $\pm 0.7\%$ on ω corresponds to the following uncertainty for each of the measurements:

$$\Delta\rho_i(\omega) = \pm 0.007 \frac{6.4\%}{10.0\%} \rho(H_i)$$

The latter results are shown in Table 4.3.

Table 4.3. Calculated reactivity ρ_{calc} [pcm] and discrepancy of each participant's result against the mean value [pcm], and uncertainty due to the measured inverse period [pcm]

Results	Case 2 H ₂	Case 3 H ₃	Case 4 H ₄	Case 5 Boron	Case 6 Erbium
Mean	88.4	109.6	130.5	83.8	169.6
HEXNOD	88.3-0.1	109.3-0.3	130.3-0.2	–	–
MCU	88.4+0.0	109.5-0.1	130.6+0.1	85.0+1.2	179.5+9.9
HELIOS	89.2+0.8	110.9+1.3	132.3+1.8	81.3-2.5	163.8-5.8
BOXER	87.8-0.6	108.6-1.0	129.0-1.5	85.1+1.3	165.4-4.2
$\Delta\rho_i(\omega)$	± 0.40	± 0.49	± 0.58	± 0.38	± 0.76

Assuming the different inaccuracies are independent from each other, the total uncertainty of the “kinetics” reactivity values is given as the square root of the sum of the quadratic value of each individual term (see also Section 2.1.5). They are reproduced as $\Delta\rho_{kin}$ in Table 4.4. They can be assumed to represent one standard deviation (1σ). The second term largely dominates the uncertainty; for Cases 2 to 4 it represents a maximum possible deviation. For those cases, assuming 1σ for $\Delta\rho_{kin}$ is therefore largely conservative.

For the three cases with increased water level (configurations H₂, H₃ and H₄), the reactivity values are in good agreement, which was to be expected considering the good consistency in the multiplication factors indicated in Table 4.1. The differences are larger in Case 5, probably reflecting the fact that it is not very easy to model the central absorber rod. They are still a little larger in Case 6, where the basic cross-sections of the erbium isotopes may play a role, as well as the resonance shielding calculations for these isotopes. Because of the good consistency of the calculated reactivity values for all methods (at least for Cases 2 to 4), these values can be taken as references for the “kinetics” reactivity values.

4.6.3 “Kinetics” reactivity effects

The point kinetics parameters calculated by the different participants were used with the measured inverse reactor period ω to determine the reactivity using the Inhour equation:

$$\rho_{kin} [\text{pcm}] = 10^5 \cdot \left(\Lambda \cdot \omega + \sum_{i=1}^6 \frac{\beta_i \cdot \omega}{\lambda_i + \omega} \right)$$

where Λ is the calculated neutron generation time [sec], λ_i is the decay factors in the six precursor groups [sec⁻¹], β_i is the calculated effective delayed neutron fraction in each precursor group and ω is the measured inverse reactor period [sec⁻¹].

In Table 4.4, the “kinetics” reactivity values ρ_{kin} are compared to the calculated ones ρ_{calc} for each calculation method.

Table 4.4. Total experimental uncertainty $\Delta\rho_{kin}$ [pcm], “kinetics” reactivity value ρ_{kin} [pcm] given by each calculation method, and differences to the calculated reactivity ρ_{calc} for the same method [pcm]

Method	Case 2 H ₂	Case 3 H ₃	Case 4 H ₄	Case 5 Boron	Case 6 Erbium
$\Delta\rho_{kin}$	±1.1	±1.2	±1.2	±3.4	±2.9
HEXNOD	81.8-6.5	101.8-7.5	120.8-9.5	79.2 xxxxxx	150.1 xxxxxx
MCU	88.0-0.4	109.5+0.0	129.9-0.7	85.2+0.2	161.4-18.1
HELIOS	74.2-15.0	92.5-18.4	110.0-22.3	71.8-9.5	137.2-26.6
BOXER	88.9+1.1	110.6+2.0	131.2+2.2	86.1+1.0	163.0-2.4

xxxxxx: The corresponding ρ_{calc} values were not provided.

First, it is interesting to note that most of the “kinetics” reactivity values are smaller than the corresponding calculated values, and it seems that the differences increase with the value of the inverse reactor period. Then, particularly for HELIOS and in a smaller measure also for HEXNOD, the calculated kinetics parameters fairly strongly underestimate the reactivity. On the contrary, MCU and BOXER show a good agreement between each other and also between both calculated and “kinetics” reactivity values. The discrepancies of the results from these two calculation methods are not far from the uncertainty of the period measurements given as $\Delta\rho_{kin}$.

Note about the MCU results for Cases 5 and 6: The statistical uncertainty σ of ρ_{calc} for Case 5 (see Table 4.3) is 13%, and it is 6% for Case 6, what corresponds to ±11 pcm for both cases. Therefore the agreement is very good for Case 5 where the difference is only 0.2 pcm; it is still acceptable for Case 6 because the discrepancy of 18 pcm is less than 2 σ .

When the calculated reactivities ρ_{calc} are considered as reference values, it is possible, for each calculation method, to recalculate the inverse reactor period ω_{calc} which gives the same reactivity when the Inhour equation is based on the kinetics parameters of the same method. This was done by inverting the Inhour equation with the Newton's method:

$$f \cong f(x_0) + (x_1 - x_0) \frac{df(x=x_0)}{dx}$$

The value of the function f is known (it is ρ_{calc} for the method considered). x_0 is a first approximation of the searched root, and x_1 is a better approximation obtained as:

$$x_1 = x_0 + (f - f(x_0)) / \frac{df(x=x_0)}{dx}$$

As a first approximation, the measured inverse period (Tables 1.5 and 1.6) was used. Then the same equation is iteratively used until the convergence is reached. It is assumed so when the relative difference between a new approximation and the former one is smaller than $1.0\text{E-}4$. In every case the convergence was reached in three iterations. Table 4.5 shows the results as ω_{calc} corresponding to ρ_{calc} , and the relative difference (%) to the measured inverse period ω_{meas} . The relative difference is to be compared with the uncertainty on ω_{meas} , which was calculated according to the formula:

$$\Delta\omega_i [\%] = 0.7\% * \Delta\rho_{\text{kin}} (\text{Table 4.4}) / \Delta\rho_i(\omega) (\text{Table 4.3})$$

Table 4.5. Comparison of the calculated inverse reactor periods for each calculation method against the measured inverse periods ω_{meas} (the discrepancies are given in %)

	Case 2 H₂	Case 3 H₃	Case 4 H₄	Case 5 Boron	Case 6 Erbium
$\omega_{\text{meas}} [\text{sec}^{-1}]$	1.3422E-2	1.8180E-2	2.3392E-2	1.2856E-2	3.2976E-2
$\Delta\omega_i [\%]$	± 1.9	± 1.7	± 1.4	± 6.3	± 2.7
HEXNOD ^(a)	1.4887E-2 +10.9%	2.0152E-2 +10.8%	2.6289E-2 +12.4%	1.3861E-2 +7.8%	4.0568E-2 +23.0%
MCU	1.3512E-2 +0.7%	1.8184E-2 +0.0%	2.3581E-2 +0.8%	1.2827E-2 -0.3%	3.9447E-2 +19.6%
HELIOS	1.7260E-2 +28.6%	2.3665E-2 +30.2%	3.1090E-2 +32.9%	1.5181E-2 +18.1%	4.4339E-2 +34.5%
BOXER	1.3196E-2 -1.7%	1.7706E-2 -2.6%	2.2792E-2 -2.6%	1.2657E-2 -1.5%	3.3767E-2 +2.4%

^(a) For Cases 5 and 6 the calculated reactivity is taken as the "mean" from Table 4.3.

The results obtained by MCU are all in the uncertainty range of the reference inverse period ω_{meas} until the last one for Case 6 (see notice above). The agreement is also good for BOXER where three results are in the uncertainty range, the two other being less than 2σ away from the reference value. The discrepancies are larger with HEXNOD, being between 5 and 9σ from the reference values. They are still much larger with HELIOS.

In the hope of obtaining more information about the origin of the differences, a detailed analysis of the results for the configuration H₄ has been undertaken. Table 4.6 shows the value of each term of

Table 4.6. Comparison of the values of the seven terms of the Inhour equation for all participants [pcm] for configuration H₄ (the factor 10⁵ is included)

Term, i	$\Lambda^*\omega$	1	2	3	4	5	6
Mean	0.14	15.67	62.13	22.37	20.45	2.21	0.24
HEXNOD	0.13	15.91	61.31	21.71	19.89	1.68	0.14
MCU	0.14	14.59	67.61	24.78	21.28	2.16	0.27
HELIOS	0.14	14.71	53.24	19.37	19.02	3.17	0.40
BOXER	0.14	17.46	66.36	23.64	21.63	1.84	0.16

the Inhour equation from each calculation method. The largest differences are observed in the precursor Groups 2 and 3 between HELIOS and MCU. The good consistency between MCU and BOXER in ρ_{kin} is partly due to compensations between the values in the Groups 1 to 3.

The last test consists in arbitrarily increasing the value of the inverse period ω and comparing the variation of the different terms of ρ_{kin} . A 10% increase of ω produces a systematic increase of 6.4% for ρ_{kin} for all participants. As Table 4.7 shows, the increase of the “kinetics” reactivity depends on the considered term, increasing from about 3% for the first precursor group to about 10% in the sixth one, but the difference is almost the same for all calculation methods (the variations observed for the sixth term are due to a loss of digits).

Table 4.7. Variation [%] of the partial values of the “kinetics” reactivity in the precursor Groups 1 to 6 due to a 10% increase of the inverse reactor period ω for the configuration H₄

Group	1	2	3	4	5	6
HEXNOD	3.3	5.5	8.2	9.2	10.1	14
MCU	3.2	5.4	8.2	9.3	9.7	11
HELIOS	3.5	5.5	8.3	9.2	9.8	10
BOXER	3.3	5.5	8.2	9.2	9.8	6

4.7 Results of reaction rate distribution calculations

Reaction rate distribution measurements were not performed.

4.8 Results of power distribution calculations

Power distribution measurements were not performed.

4.9 Results of isotopic calculations

Isotopic measurements were not performed.

4.10 Results of calculations for other miscellaneous types of measurements

Other miscellaneous types of calculations were not performed.

REFERENCES

- [1] Früh, R., *Réacteur CROCUS, Complément au rapport de sécurité: Réactivité et paramètres cinétiques*, LPR 196, EPFL Lausanne, December 1993.
- [2] Pralong, C., *et al.*, “Reactivity Effects of Burnable Poisons Proposed for Pu-incinerating LWR Fuels”, *Proc. ICENES’98*, Tel Aviv, June/July 1998.
- [3] Weast, R.C., M.J. Astle, “CRC Handbook of Chemistry and Physics”, p. F-11, 60th Edition, CRC Press, Boca Raton, Florida (1980).
- [4] Pfennig, G., H. Klewe-Nebenius, W. Seelmann-Eggebert, *Karlsruher Nuklidkarte*, Forschungszentrum Karlsruhe, November 1995.
- [5] Keepin, G.R., “Asymptotic Period-reactivity Relations”, Chapter 7 in *Physics of Nuclear Kinetics*, p. 187, Addison Wesley Publishing Company (1965).

Appendix A

COMPUTER CODES, CROSS-SECTIONS AND TYPICAL INPUT LISTINGS

A.1 Name(s) of code system(s) used

HEXNOD: HEXNOD is a deterministic 2-D/3-D transport code, its group constants being prepared by CASMO-4.

MCU: Pointwise Monte Carlo code MCU-REA used in two dimensions (some results were obtained using three dimensions).

HELIOS: HELIOS is a general 2-D neutron physics transport code applicable to almost every 2-D configuration.

BOXER: BOXER is a cell and 2-D transport code in X-Y geometry.

A.2 Bibliographic references for the codes used

HEXNOD:

Wagner, M.R., "Three-dimensional Nodal Diffusion and Transport Methods for Hexagonal-Z Geometry", *Nucl. Sc. Eng.*, 103, 377 (1989).

Takeda, T., H. Ikeda, *3-D Neutron Transport Benchmarks*, OECD/NEA Committee on Reactor Physics, NEACRP-L-330.

Lieberoth, J., "A Monte Carlo Technique to Solve the Static Eigenvalue Problem of the Boltzmann Transport Equation", *Nukleonik*, 11, 213-219 (1968).

MCU:

Abagjan, L.P., N.I. Alexeyev, V.I. Bryzgalov, "The Use of the Codes from MCU Family for Calculations of VVER Type Reactors", *Proceedings of the 10th AER International Topical Meeting*, Moscow, Russia, 18-22 September 2000.

Mayorov, L., V. Zolotukhin, "The Estimation of Criticality Parameters by Monte Carlo Method", *Energoatomizdat*, Moscow (1984) (in Russian).

Mayorov, L., "Monte Carlo Codes and Applications", Chapter 3 in *Theoretical Investigations of the Physical Properties of WWER-type Uranium-water Lattices*, Vol. 2, pg. 70, Akademiai Kiado, Budapest (1994).

HELIOS:

Casal, J.J., R.J.J. Stamm'ler, E.A. Villarino, A.A. Ferri, "HELIOS: Geometric Capabilities of a New Fuel-assembly Program", *Int. Topical Meeting on Advances in Mathematics, Computations and Reactor Physics*, Pittsburgh, USA (1991).

Villarino, E.A., R.J.J. Stamm'ler, "HELIOS: Transformation Laws for Multiple-collision Probabilities with Angular Dependence", *Int. Conf. on Physics of Reactors PHYSOR 96*, Mito, Japan (1996).

BOXER:

Paratte, J.M., K. Foskolos, P. Grimm, J.M. Hollard, *ELCOS – the PSI Code System for LWR Core Analysis. Part I: User’s Manual for the Library Preparation Code ETOBOX*, PSI Bericht Nr. 96-02 (January 1996).

Paratte, J.M., P. Grimm, J.M. Hollard, *ELCOS – the PSI Code System for LWR Core Analysis. Part II: User’s Manual for the Fuel Assembly Code BOXER*, PSI Bericht Nr.96-08 (February 1996).

A.3 Origin of cross-section data

HEXNOD: L-Lib for CASMO-4 based mainly on ENDF/B.

MCU: The cross-section library used by the code is called MCUDAT2.1. It is based on ENDF/B-6, JENDL-3.2 and BROND. The basic libraries are processed by LIPAR for the parameters of the resolved resonances, KORT for the resonance integrals at 0.0253 eV, and BFS for the treatment of the $S(\alpha,\beta)$ matrices. The kinetics parameters are taken from ABBN-93.

HELIOS: Standard HELIOS library in 45 energy groups.

BOXER: The library used by BOXER is called LIBRAN. This library is produced by the code ETOBOX on the basis of JEF-1 and on BROND-2 for erbium isotopes.

A.4 Spectral calculations and data reduction methods used

N/A

A.5 Number of energy groups or continuous energy used in the different phases of the calculation

HEXNOD: The CASMO cell calculation uses 40 groups, which are condensed to 5 groups for the 2-D calculations.

MCU: The code uses a pointwise description of the energy during the entire calculation.

HELIOS: The 2-D calculation is done in 45 energy groups. For the condensation of the kinetics parameters, a 12-group structure was used.

BOXER: At the beginning of the cell calculation, the pointwise spectrum is determined in two material zones and about 8 000 lethargy points (between 1.3 and 907 eV) in order to condense the resonance cross-sections into groups. Afterwards, the cell calculation itself is performed in one dimension and 70 energy groups. The 2-D calculations of the core were also done in 70 energy groups.

A.6 Cell calculation

HEXNOD: Cell calculations were performed with CASMO-4. The cell dimensions of the oxide cells were enlarged to take into account the water slabs between the oxide and the metallic regions. Forty (40) energy groups are used for cell calculations; they are condensed to 5 groups for the 2-D and 3-D calculations.

MCU: A cell calculation is not explicitly done (it is included in the calculation of the whole configuration).

HELIOS: The cell calculation is not separated from the overall 2-D calculation. The discretisation of the partial currents between structures is defined by the coupling order. For the CROCUS calculation, the standard coupling number $k = 4$ was used.

BOXER: Cell calculations are performed in one-dimensional transport theory and 70 energy groups in order to condense the geometry of the cells.

A.7 Other assumptions and characteristics

HEXNOD: The water slabs between the two zones of the reactor (oxide and metallic fuel) are homogenised with the moderator region of the oxide cells. The CASMO values for the delayed neutrons in each zone are condensed with the neutron production rate from the 2-D calculation as weighting function. The neutron generation time is calculated in MOCA with the inverse velocities in each CASMO group as input.

MCU: The 2-D model is based on the benchmark specification without any approximation, the Z-direction being replaced by the given bucklings. In the 3-D model, the configuration is axially limited by the two Cd layers which are replaced here by black boundary conditions. The effective delayed neutron fraction is calculated through the following formula:

$$\beta_{eff} = \frac{k_{eff} - k_{prompt}}{k_{eff}}$$

where k_{eff} is the effective multiplication factor with delayed neutrons being taken into account and k_{prompt} is the effective multiplication factor with only prompt neutrons being taken into account.

HELIOS: The kinetics parameters given by HELIOS were calculated using the methodology proposed by R. Stamm'ler in the user's manual of HELIOS (SSP method in the module ZENITH). The β -values are condensed over groups using the production as weighting function in each group and each zone to get the effective one-group β_{eff} .

BOXER: During the cell calculation, the kinetics parameters are determined by integration with the importance function (direct flux times adjoint flux) after spatial condensation of the cell regions. In the 2-D calculations, the kinetics parameters are condensed with the power distribution as weighting function.

A.8 Typical input listings for each code system type

A.8.1 BOXER input for CROCUS with varying water level

```
*Crocus, 1/4 coeur: Variation de la hauteur d'eau. Hcrit, BZ2=9.0900-4cm-2
iniact=32000,
CALL (DEFINE, CELL, MACRO, TWODIM(CODIFF,QP1), GENCOR)
OPTIONS (IMA=44,44,44,44,LSYM=1,LLB=2,LTB=2,LRB=3,LBB=3, NOUTIT=200,
        TOLKEFF=1.0E-7,1.0E-6, TWODBUCK=9.0900E-4, ALBEDO=0.0, KINETICS=1,
        CELLBUCK=5.34E-3, TOLCTH=1.0E-4, TOLCF=1.0E-4)
PRINTOUT (MICOND=2, CRITA=2, GENCOR=2, NG3CROSS=0,
        NG4CROSS=0, MACRO=1, TWODFL=0, TWODPO=1, MATPOW=1, MATREA=1)
MATERIAL (1, FUEL, D=10.556, PART=1, LIST=92235,1.806,92238,98.194)
MATERIAL (2, CLAD, FUELD=1.052,CLADTH=0.085,CLADOD=1.26,LIST=13027,2.70)
MATERIAL (3, WATER)
MATERIAL (3, SAME=4)
MATERIAL (11,FUEL,TYPE=METAL, D=18.677, PART=1,LIST=92235,0.947,92238,99.053)
MATERIAL (12,CLAD,FUELD=1.70, CLADTH=0.1, CLADOD=1.935, LIST=13027,2.70)
CELLTYPE (1, NQTH=2, NASTH=1, NQF=2,
        MICRO=1,1,2,2,3,3, RAD=0.526,1,0.63,2, SQUARE=1.837)
CELLTYPE (11, NQTH=2, NASTH=1, NQF=2, DANCOF=0.9091, INFINITE,
        MICRO=1,1,2,2,3,3, RAD=0.85,1,0.9675,2, SQUARE=2.917)
HETERO (MAT(1,TYPE=1,MICRO=1,2,3), MAT(11,TYPE=11,MICRO=11,12,3))
GROUPS (NG2=70,33,1,1)
GROUPS (NG3=70,33,1,1)
GROUPS (NG4=2,1,0,0, FINEGR=33,70)

/GROUPS (NG2=15,9,1,1, FINEGR=3,6,13,20,23,26,27,28,33,37,46,51,56,63,70)
/GROUPS (NG3=15,9,1,1)
/GROUPS (NG4=2,1,0,0, FINEGR=9,15)

GEOMETRY (BOXOL, ARRAY= 4,0,44,0,44, 3,0,27,0,27,
        1,0,6,0,26, 1,6,14,0,22, 1,14,22,0,14, 1,22,26,0,6,
        11,27,36,0,7, 11,23,36,7,11, 11,23,33,11,15, 11,15,33,15,19,
        11,15,30,19,23, 11,7,30,23,27, 11,0,26,27,30, 11,0,19,30,33,
        11,0,11,33,36,
        meshes=0.9185,2,1.080,3,0.757,4,0.9185,6,0.323,7,.757,9,.7015,11,.434,12,
        .9185,14,.646,15,.5955,17,.863,19,.111,20,.9185,22,.969,23,
        .868,24,.9185,26,.212,27,.972333,36,1.0,40,2.0,42,5.0,44)
GEOMETRY (TWODIM=BOXOL)
GEOMETRY (MEANS=BOXOL)
WEIGHTS (NG2)
WEIGHTS (NG3)
END (DEFINE)
*Crocus, 1/4 coeur: Variation de la hauteur d'eau. H2, BZ2=8.8222-4cm-2
CALL (DEFINE, TWODIM(QP1), GENCOR)
OPTIONS (TWODBUCK=8.8222E-4)
END (DEFINE)
*Crocus, 1/4 coeur: Variation de la hauteur d'eau. H3, BZ2=8.7591-4cm-2
CALL (DEFINE, TWODIM(QP1), GENCOR)
OPTIONS (TWODBUCK=8.759E-4)
END (DEFINE)
*Crocus, 1/4 coeur: Variation de la hauteur d'eau. H4, BZ2=8.6967-4cm-2
CALL (DEFINE, TWODIM(QP1), GENCOR)
OPTIONS (TWODBUCK=8.6967E-4)
END (DEFINE)
END (BOXER)
```

A.8.2 BOXER input for CROCUS for absorption rods at the center of core

```
*Crocus-Case 5.a, 1/1 coeur: Boron rod, bukling search.
iniact=32000,
CALL (DEFINE, CELL, MACRO, TWODIM(CODIFF,QP1), GENCOR)
OPTIONS (IMA=90,90,90,90,LSYM=0,LLB=3,LTB=3,LRB=3,LBB=3, LSEARCH=3, NOUITIT=200,
        KINETICS=1,TOLKEFF=1.0E-7,1.0E-4, TWODBUCK=8.0E-4, ALBEDO=0.0,
        CELLBUCK=5.34E-3, TOLCTH=1.0E-4, TOLCF=1.0E-4)
PRINTOUT (MICOND=2, CRITA=2, GENCOR=2, NG3CROSS=0,
         NG4CROSS=0, MACRO=1, TWODFL=0, TWODPO=1, MATPOW=1, MATREA=1)
MATERIAL (1, FUEL, D=10.556, PART=1, LIST=92235,1.806,92238,98.194)
MATERIAL (2, CLAD, FUELD=1.052,CLADTH=0.085,CLADOD=1.26,LIST=13027,2.70)
MATERIAL (3, WATER)
MATERIAL (3, SAME=4)
MATERIAL (11,FUEL,TYPE=METAL, D=18.677, PART=1,LIST=92235,0.947,92238,99.053)
MATERIAL (12,CLAD,FUELD=1.70, CLADTH=0.1, CLADOD=1.935, LIST=13027,2.70)
/Tube Umetal rempli d'eau - mat 5:
MATERIAL (30,ISOTOPE,LIST=13027,2.70) / Aluminium
MATERIAL (5, MIXTURE=30,0.18350,3,8.32539)
/ Barreau absorbant, 6768 ppm Bnat - mat 6 (adjonction de traces de Zr pour
/ le calcul en SLOFIN):
MATERIAL (6, WATER, PPM=5000,6768, UNIT=ATOMS, OTHERS=40001,1.0-9)
/Cellules combustibles entourant le barreau absorbant:
CELLTYPE (2, MICRO=1,1,2,2,3,3, RAD=0.526,1,0.63,2, SQUARE=1.431565)
/Cellule du barreau absorbant:
CELLTYPE (6, DANCOF=1, MICRO=1,1,2,2,3,3, RAD=0.3,1,0.4,2,0.649478,3)
/Cellules combustibles:
CELLTYPE (1, INFINITE, MICRO=1,1,2,2,3,3, RAD=0.526,1,0.63,2, SQUARE=1.837)
CELLTYPE (11, DANCOF=0.9091, INFINITE,
         MICRO=1,1,2,2,3,3, RAD=0.85,1,0.9675,2, SQUARE=2.917)
HETERO (MAT(1,TYPE=1,MICRO=1,2,3), MAT(11,TYPE=11,MICRO=11,12,3),
        MAT(2,TYPE=2,MICRO=1,2,3), MAT(6, TYPE=6,MICRO=6,30,3))
GROUPS (NG2=70,33,1,1)
GROUPS (NG3=70,33,1,1)
GROUPS (NG4=2,1,0,0, FINEGR=33,70)

/GROUPS (NG2=15,9,1,1, FINEGR=3,6,13,20,23,26,27,28,33,37,46,51,56,63,70)
/GROUPS (NG3=15,9,1,1)
/GROUPS (NG4=2,1,0,0, FINEGR=9,15)

GEOMETRY (BOXOL, ARRAY= 4,0,90,0,90, 3,17,73,17,73,
         11,8,11,33,57, 11,11,14,21,65, 11,14,17,17,73, 11,17,21,14,37,
         11,17,21,53,76, 11,21,25,11,29, 11,21,25,61,76, 11,25,29,11,29,
         11,25,29,61,79, 11,29,33,8,21, 11,29,33,69,79, 11,33,37,8,21,
         11,33,37,69,82, 11,37,53,8,17, 11,37,53,73,82, 11,53,57,8,21,
         11,53,57,69,82, 11,57,61,11,21, 11,57,61,69,82, 11,61,65,11,29,
         11,61,65,61,79, 11,65,69,14,29, 11,65,69,61,79, 11,69,73,14,37,
         11,69,73,53,76, 11,73,76,17,73, 11,76,79,25,69, 11,79,82,33,57,
         1,18,22,38,52, 1,22,30,30,60, 1,30,38,22,68, 1,38,52,18,72,
         1,52,60,22,68, 1,60,68,30,60, 1,68,72,38,52,
         2,43,47,43,47, 6,44,46,44,46, 5,21,25,21,25, 5,65,69,65,69,
         meshes=5.0,2,2.0,4,1.0,8,.972333,17,.212,18,.9185,20,.868,21,.969,22,
         .9185,24,.111,25,.863,27,.5955,29,.646,30,.9185,32,.434,33,
         .7015,35,.757,37,0.323,38,0.9185,40,0.757,41,1.080,42,0.9185,43,
         .342916,44,
         .575585,46,.342916,47,0.9185,48,1.080,49,0.757,50,0.9185,52,0.323,53,
         .757,55,.7015,57,.434,58,
         .9185,60,.646,61,.5955,63,.863,65,.111,66,.9185,68,.969,69,
         .868,70,.9185,72,.212,73,.972333,82,1.0,86,2.0,88,5.0,90)
GEOMETRY (TWODIM=BOXOL)
WEIGHTS (NG2)
WEIGHTS (NG3)
END(DEFINE)
*Crocus-Case 5.b, 1/1 coeur: Withdraw of boron rod, Fixed buckling.
CALL (DEFINE, TWODIM(QP1), GENCOR)
OPTIONS (LSEARCH=1)
GEOMETRY (BOXOL, ARRAY=1,43,47,43,47)
GEOMETRY (TWODIM=BOXOL)
END(DEFINE)
*Crocus-Case 6.a, 1/1 coeur: Erbium rod, buckling search.
```

```

CALL (DEFINE, CELL, MACRO, TWODIM(QP1), GENCOR)
OPTIONS (LSEARCH=3, KEFF=1.0)
MATERIAL (6, FUEL, DENSITY=4.594, DR=TOTAL,
          TYPE=MO2, PART=0.809752, LIST=40001,100,
          TYPE=M2O3, PART=0.190248, UNIT=APC,
          LIST=468162,0.14,468164,1.61,468166,33.6,468167,22.95,468168,26.8,
          468170,14.9)
MATERIAL (7,CLAD,FUELD=0.589, CLADTH=0.1, CLADOD=0.8, LIST=13027,2.70)
/Cellule du barreau absorbant:
CELLTYPE (6, DANCOF=1, MICRO=1,1,2,2,3,3, RAD=0.2945,1,0.4,2,0.649478,3)
HETERO (MAT(1,TYPE=1,MICRO=1,2,3), MAT(11,TYPE=11,MICRO=11,12,3),
        MAT(2,TYPE=2,MICRO=1,2,3), MAT(6, TYPE=6,MICRO=6,7,3))
GEOMETRY (BOXOL, ARRAY=2,43,47,43,47, 6,44,46,44,46)
GEOMETRY (TWODIM=BOXOL)
END(DEFINE)
*Crocus-Case 6.b, 1/1 coeur: Withdraw of erbium rod, Fixed buckling.
CALL (DEFINE, TWODIM(QP1), GENCOR)
OPTIONS (LSEARCH=1)
GEOMETRY (BOXOL, ARRAY=1,43,47,43,47)
GEOMETRY (TWODIM=BOXOL)
END(DEFINE)
/
END (BOXER)

```


A.8.3 CASMO-4 input metal zone

```
TIT *crocus metal zone 0.95% U-235
TFU=293 * fuel temperat. in K
TMO=293 * moderator temp in K
VOI=00
THE 0
* -----
* fuel dens. 18.68 metal/ cladding = aluminium
*
FUE 1 18.677 0 /0.947 8000=0.0
CAN 2.70 0 /13000=100.0
* -----
*
PDQ 'BND' 1 0 1 -3 // 92235, 92236, 92238, 94239, 94240, 94241, 94242, 95241
54135, 62149, 93237, 94238, 92234
*
* Sidepins Pitch box-ID wall Gap wide/narrow
PWR 2 2.917 5.834 0. 0. 0. 0 2
*
* pellet out clad inner clad outer
PIN 1 0.85 0.8675 0.9675
*
LPI
1
1 1
LFU
1
1 1
*
PDE 0.0 * pow dens in W/gU
PRI 10*0 1
CON //5 9 15 28 40//5 9 15 28 40
* GRP
AVE 'CELL' /0 0 1 0 0 1 0 0 1
PUN 6*0 2 0 0 0 0 1
* PUN 9*0 1*
DEP 0.
WRI 0 / 'CIF' 'OUT' 'RES'
STA
END
TIT *crocus metal zone 0.95% U-235
```

A.8.4 CASMO-4 input oxide zone

```

TIT *crocus oxide zone 1.8% U-235
TFU=293 * Brennstofftemp. in K
TMO=293 * Moderatortemp. in K
VOI=00
THE 0
*
* -----
* density 10.55 oxide / clad = aluminium
*
FUE 1 10.556 0 /1.8060
CAN 2.70 0 /13000=100.0
* -----
*
PDQ 'BND' 1 0 1 -3 // 92235, 92236, 92238, 94239, 94240, 94241, 94242, 95241
54135, 62149, 93237, 94238, 92234
* pitch adjusted from 1.837 to 1.85025
* Sidepins Pitch Box-ID wall thickn. Gap wide/narrow
PWR 2 1.85025 3.7005 0. 0. 0. 0 2
*
* pellet clad-inner clad-outer
PIN 1 0.526 0.545 0.63
*
LPI
1
1 1
LFU
1
1 1
*
PDE 0.0 * power dens in W/gU
PRI 10*0 1
CON //5 9 15 28 40//5 9 15 28 40
* GRP
AVE 'CELL' /0 0 1 0 0 1 0 0 1
PUN 6*0 2 0 0 0 0 1
* PUN 9*0 1
*
DEP 0.
WRI 0 / 'CIF' 'OUT' 'RES'
STA
END

```

3 CASMO-4 Results:

REGION	casmo-4 k_{eff}
metal-zone	1.08032
oxide-zone	1.24640

A.8.5 HEXNOD input 2-D

```

**TEXT
  SIMPLIFIED 2d crocus (hexagonal mockup) 1/6 core rot. sym
  casmo-4 X-sec 5 GR, nodal transport ,13 ROWS ,1 LAYER (2D)
  hex pitch 2.9086 cm , X-sec from data file "crc405g.wq"
**DATA
  2 5 20 1 1 3 3 40 0 1 1 1 1 0 -1 1
  4 10 1 2 1 0
1000.0      0.32044 -10 0.5      -4
2.9086
10.
  1
**HEX
      1
    1
  1 1
1 1 1
 1 1 1 1
 1 1 1 1 1
 2 1 1 1 1 1 2
 2 2 3 2 2 3 2 2
 2 2 2 2 2 2 2 2 2
 3 3 3 3 3 3 3 3 3
 3 3 3 3 3 3 3 3 3 3
 3 3 3 3 3 3 3 3 3 3 3
 3 3 3 3 3 3 3 3 3 3 3 3
 3 3 3 3 3 3 3 3 3 3 3 3 3
 3 3 3 3 3 3 3 3 3 3 3 3 3 3
 3 3 3 3 3 3 3 3 3 3 3 3 3 3 3
 3 3 3 3 3 3 3 3 3 3 3 3 3 3 3 3
**COLUMN
oxide 1
      1 1
      1 2
metal  2
      1 2
      1 2
water  3
      1 3
      1 2
**MAT
  4 2 3
  4 1 0 0 0
READ_FILE
crc405g.wq
READ_FILE
crc405g.wq
READ_FILE
crc405g.wq

```

A.8.6 HEXNOD input 3-D

```

**TEXT
SIMPLIFIED 3d crocus (hexagonal mockup) 1/6 core rot. sym.
casmo-4 X-sec 5 GR, nodal transport, 13 ROWS, 20 LAYERS (3D), 18 Mat.
100 cm core, vac.bound.cond. top/bottom, hex pitch 2.9086 cm, X-sec from data file
"crok5st.wq"
**DATA
  3  5 20  1 20 18  3 40  0  0  0  1  1  0 -1 20
  4  4  1  2  1  0
1000.0      0.32044 -10 0.5      -4
2.9086
14.3 3.0 2.15 0.55 0.5 9.5 10.0 10.0 10. 10.0 10.0 10.0 10.0 10.0 6.51 3.49 0.5
0.55 1.50 15.0
  1  1  1  1  1  1  1  1  1  1  1  1  1  1  1  1  1  1  1
**HEX
      1
    1 1
  1 1 1
1 1 1 1
  1 1 1 1 1
    2 1 1 1 1 1 2
      2 2 3 2 2 3 2 2
        2 2 2 2 2 2 2 2
          2 2 2 2 2 2 2 2
            3 3 3 2 2 2 2 2 3 3
              3 3 3 3 3 3 3 3 3 3
                3 3 3 3 3 3 3 3 3 3
                  3 3 3 3 3 3 3 3 3
                    3 3 3 3 3 3 3 3 3
                      3 3 3 3 3 3 3 3
                        3 3 3 3 3 3 3 3
                          3 3 3 3 3 3 3 3
                            3 3 3 3 3 3 3 3
                              3 3 3 3 3 3 3 3
                                3 3 3 3 3 3 3 3
                                  3 3 3 3 3 3 3 3
**COLUMN
oxide  1
      11 16 13  7 11 17  1  5 14 11 13  9
      1  2  3  4  5  6 16 17 18 19 20 21
metal  2
      11 16 13  8 12 18  2  6 15 12 13 10
      1  2  3  4  5  6 16 17 18 19 20 21
water  3
      4 16 12  3 15
      1  4  5 16 21
**MAT
  1  2  3  4  5  6  7  8  9 10 11 12 13 14 15 16 17 18
18  0  0  0  0
READ_FILE
crok5st.wq
READ_FILE
crok5st.wq

```

A.8.7 MCU input

A.8.7.1 2-D cases 1,2,3,4: Hkrit, H₂,H₃,H₄

```

                                                    TEMPR* 300.0
FZONE* 1
U235: 4.3056E-04
U238: 2.3114E-02
O   : 4.7089E-02
FZONE* 2
U235: 4.5316E-04
U238: 4.6801E-02
FZONE* 3
AL  : 6.0262E-02
FZONE* 4
HE4 : 2.4675E-05
FZONE* 5
H   : 6.6742E-02
O   : 3.3371E-02
FZONE* 6
H   : 6.6742E-02
O   : 3.3371E-02
FZONE* 7
CD  : 4.6340E-02
FZONE* 8
FE  : 5.9873E-02
CR  : 1.6298E-02
NI  : 7.2342E-03
MN  : 1.7022E-03
FZONE* 9
H   : 6.6742E-02
O   : 3.3371E-02
B10 : 7.4892E-05
B11 : 3.0147E-04
FZONE* 10
ER  : 3.1144E-02
FINISH MAT
HEAD 1 0 2000
CONT T T B
EQU  HALL = 1.0
**   UO2 TVEL
EQU  RCLAD2 = 0.630
EQU  RCLAD1 = 0.545
EQU  RFUEL  = 0.526
EQU  P      = 1.837
**   U METAL
EQU  MCLAD2 = 0.9675
EQU  MCLAD1 = 0.8675
EQU  MFUEL  = 0.85
*   MAIN ELEMENT
RCZ  N1  0. 0. 0.          HALL      65.0
RPP  N2  -3*P 3*P -11*P 11*P 0 HALL
RPP  N3  -6*P 6*P -9*P 9*P 0 HALL
RPP  N4  -9*P 9*P -6*P 6*P 0 HALL
RPP  N5  -11*P 11*P -3*P 3*P 0 HALL
END
Z1 (LT1) 1 -2 -3 -4 -5 /6:6/6
Z2 (LT)  2 U 3 U 4 U 5 /6:6/6
END
#####
**   UO2 CELL
CELL X
SBOX N1 1.837, 0., 0., 0., 1.837, 0., 0., 0., HALL
*   CLAD
RCZ  N2  0.9185 0.9185 0.0 HALL RCLAD2
RCZ  N3  0.9185 0.9185 0.0 HALL RCLAD1
*   MAIN CYLINDERS
RCZ  N4  0.9185 0.9185 0.0 HALL RFUEL
END
```

```

WATR      1  -2                      /5:5/1
CLAD      2  -3                      /3:3/1
AIR       3  -4                      /4:4/1
FUEL     4
END

```

```

#####

```

```

**      U METAL
CELL    Y
SBOX    N1  2.917, 0., 0., 0., 2.917, 0., 0., 0., HALL
*      CLAD
RCZ     N2  1.4585 1.4585 0.0    HALL    MCLAD2
RCZ     N3  1.4585 1.4585 0.0    HALL    MCLAD1
*      MAIN CYLINDERS
RCZ     N4  1.4585 1.4585 0.0    HALL    MFUEL
END

```

```

WATR      1  -2                      /5:5/2
CLAD      2  -3                      /3:3/2
AIR       3  -4                      /4:4/2
FUEL     4                      /2:2/2
END

```

```

#####

```

```

NET      LT   -20.207 -20.207 0.    22, 22
C=
C=      1 2 3 4 5 6 7 8 9 0 1 2 3 4 5 6 7 8 9 0 1 2
C=
T01     0 0 0 0 0 0 0 0 0 X X X X X 0 0 0 0 0 0 0 0 0 0
T02     0 0 0 0 0 0 0 0 0 X X X X X X 0 0 0 0 0 0 0 0
T03     0 0 0 0 0 0 X X X X X X X X X X X X 0 0 0 0 0
T04     0 0 0 0 0 X X X X X X X X X X X X 0 0 0 0 0
T05     0 0 0 0 0 X X X X X X X X X X X X 0 0 0 0 0
T06     0 0 X X X X X X X X X X X X X X X X 0 0 0 0
T07     0 0 X X X X X X X X X X X X X X X X X X 0 0
T08     0 0 X X X X X X X X X X X X X X X X X X 0 0
T09     X X X X X X X X X X X X X X X X X X X X X X
T10     X X X X X X X X X X X X X X X X X X X X X X
T11     X X X X X X X X X X X X X X X X X X X X X X
T12     X X X X X X X X X X X X X X X X X X X X X X
T13     X X X X X X X X X X X X X X X X X X X X X X
T14     X X X X X X X X X X X X X X X X X X X X X X
T15     0 0 X X X X X X X X X X X X X X X X X X 0 0
T16     0 0 X X X X X X X X X X X X X X X X X X 0 0
T17     0 0 X X X X X X X X X X X X X X X X X X 0 0
T18     0 0 0 0 0 X X X X X X X X X X X X 0 0 0 0 0
T19     0 0 0 0 0 X X X X X X X X X X X X 0 0 0 0 0
T20     0 0 0 0 0 X X X X X X X X X X X X 0 0 0 0 0
T21     0 0 0 0 0 0 0 0 X X X X X X 0 0 0 0 0 0 0 0
T22     0 0 0 0 0 0 0 0 X X X X X X 0 0 0 0 0 0 0 0
C=
C=      1 2 3 4 5 6 7 8 9 0 1 2 3 4 5 6 7 8 9 0 1 2
C=
END

```

```

#####

```

```

NET      LT1  -29.17 -29.17 0.    20, 20
C=
C=      1 2 3 4 5 6 7 8 9 0 1 2 3 4 5 6 7 8 9 0
C=
T01     0 0 0 0 0 0 0 0 Y Y Y Y Y 0 0 0 0 0 0 0 0
T02     0 0 0 0 0 Y Y Y Y Y Y Y Y Y 0 0 0 0 0 0
T03     0 0 0 Y Y Y Y Y Y Y Y Y Y Y 0 0 0 0
T04     0 0 Y Y Y Y Y Y 0 0 0 0 0 Y Y Y Y Y 0 0
T05     0 0 Y Y Y Y 0 0 0 0 0 0 0 0 0 Y Y Y Y 0 0
T06     0 Y Y Y Y Y 0 0 0 0 0 0 0 0 0 Y Y Y Y Y 0
T07     0 Y Y Y 0 0 0 0 0 0 0 0 0 0 0 0 Y Y Y 0
T08     Y Y Y Y 0 0 0 0 0 0 0 0 0 0 0 0 Y Y Y Y
T09     Y Y Y 0 0 0 0 0 0 0 0 0 0 0 0 0 0 Y Y Y
T10     Y Y Y 0 0 0 0 0 0 0 0 0 0 0 0 0 0 Y Y Y
T11     Y Y Y 0 0 0 0 0 0 0 0 0 0 0 0 0 0 Y Y Y
T12     Y Y Y 0 0 0 0 0 0 0 0 0 0 0 0 0 0 Y Y Y
T13     Y Y Y Y 0 0 0 0 0 0 0 0 0 0 0 0 0 Y Y Y
T14     0 Y Y Y 0 0 0 0 0 0 0 0 0 0 0 0 Y Y Y 0
T15     0 Y Y Y Y Y 0 0 0 0 0 0 0 0 0 Y Y Y Y Y 0

```

```

T16  0 0 Y Y Y Y 0 0 0 0 0 0 0 0 Y Y Y Y 0 0
T17  0 0 Y Y Y Y Y Y 0 0 0 0 Y Y Y Y Y Y 0 0
T18  0 0 0 Y Y Y Y Y Y Y Y Y Y Y Y Y Y 0 0 0
T19  0 0 0 0 0 Y Y Y Y Y Y Y Y Y Y 0 0 0 0 0
T20  0 0 0 0 0 0 0 Y Y Y Y Y Y 0 0 0 0 0 0 0
C=
C=   1 2 3 4 5 6 7 8 9 0 1 2 3 4 5 6 7 8 9 0
C=
END
FINISH NCG
SPNT  0.9, 0.9, 0.5
FINISH SP
ENGR  0.
NBUC  4
BUCL  0., 0., 3.01496E-02
BCRO  0.0294902 0.0295958 0.0297022 0.0301496
L
FINISH REG
NTOT  200
FINISH RUL
NAMVAR CROCUS01
MAXSER 1
DTZML 20
NPRI  200
REGZ  -1
FULL
NRAN  100
FINISH ALL

```

A.8.7.2 3-D Case 1, Hkrit

TEMPR* 300.0

```

FZONE* 1
U235: 4.3056E-04
U238: 2.3114E-02
O : 4.7089E-02
FZONE* 2
U235: 4.5316E-04
U238: 4.6801E-02
FZONE* 3
AL : 6.0262E-02
FZONE* 4
HE4 : 2.4675E-05
FZONE* 5
H : 6.6742E-02
O : 3.3371E-02
FZONE* 6
H : 6.6742E-02
O : 3.3371E-02
FZONE* 7
CD : 4.6340E-02
FZONE* 8
FE : 5.9873E-02
CR : 1.6298E-02
NI : 7.2342E-03
MN : 1.7022E-03
FZONE* 9
H : 6.6742E-02
O : 3.3371E-02
B10 : 7.4892E-05
B11 : 3.0147E-04
FZONE* 10
ER : 3.1144E-02
FZONE* 11
N : 5.4000E-05
FINISH MAT
HEAD 1 0 2000
CONT B B B
EQU HALL = 100.0
EQU HWTR = 96.51
EQU HAL = 0.5
** UO2 TVEL
EQU RCLAD2 = 0.630
EQU RCLAD1 = 0.545
EQU RFUEL = 0.526
EQU P = 1.837
** U METAL
EQU MCLAD2 = 0.9675
EQU MCLAD1 = 0.8675
EQU MFUEL = 0.85
* MAIN ELEMENT
RCZ N1 0. 0. 0. HALL 65.0
RPP N2 -3*P 3*P -11*P 11*P 0 HALL
RPP N3 -6*P 6*P -9*P 9*P 0 HALL
RPP N4 -9*P 9*P -6*P 6*P 0 HALL
RPP N5 -11*P 11*P -3*P 3*P 0 HALL
RCZ N6 0. 0. 0. HWTR 65.0
RCZ N7 0. 0. HAL HWTR-HAL 65.0
RCZ N8 0. 0. 0. HAL 65.0
END
Z1 (LT1) 1 7 -2 -3 -4 -5 /6:6/6
Z2 (LT) 7 2 U 7 3 U 7 4 U 7 5 /6:6/6
**
Z5 (LT1) 1 8 -2 -3 -4 -5 /3:3/3
Z6 (LT) 8 2 U 8 3 U 8 4 U 8 5 /3:3/3
**
Z3 (LT1) 1 -6 -2 -3 -4 -5 /11:11/7
Z4 (LT) 2 -6 U 3 -6 U 4 -6 U 5 -6 /11:11/7
END

```



```

#####
**      UO2 CELL
CELL    X
SBOX   N1   1.837, 0., 0., 0., 1.837, 0., 0., 0., HALL
*      CLAD
RCZ    N2   0.9185 0.9185 0.0   HALL   RCLAD2
RCZ    N3   0.9185 0.9185 0.0   HALL   RCLAD1
*      MAIN CYLINDERS
RCZ    N4   0.9185 0.9185 0.0   HALL   RFUEL
SBOX   N5   1.837, 0., 0., 0., 1.837, 0., 0., 0., HWTR
END
WATR   1   -2   5                               /5:5/1
WATR   1   -2  -5                               /11:11/1
CLAD   2   -3                               /3:3/1
AIR    3   -4                               /4:4/1
FUEL   4                               /1:1/1
END
#####
**      U METAL
CELL    Y
SBOX   N1   2.917, 0., 0., 0., 2.917, 0., 0., 0., HALL
*      CLAD
RCZ    N2   1.4585 1.4585 0.0   HALL   MCLAD2
RCZ    N3   1.4585 1.4585 0.0   HALL   MCLAD1
*      MAIN CYLINDERS
RCZ    N4   1.4585 1.4585 0.0   HALL   MFUEL
SBOX   N5   2.917, 0., 0., 0., 2.917, 0., 0., 0., HWTR
END
WATR   1   -2   5                               /5:5/2
WATR   1   -2  -5                               /11:11/2
CLAD   2   -3                               /3:3/2
AIR    3   -4                               /4:4/2
FUEL   4                               /2:2/2
END
#####
NET     LT   -20.207 -20.207 0.    22, 22
C=
C=      1 2 3 4 5 6 7 8 9 0 1 2 3 4 5 6 7 8 9 0 1 2
C=
T01    0 0 0 0 0 0 0 0 0 X X X X X 0 0 0 0 0 0 0 0
T02    0 0 0 0 0 0 0 0 0 X X X X X 0 0 0 0 0 0 0 0
T03    0 0 0 0 0 X X X X X X X X X X X 0 0 0 0 0 0
T04    0 0 0 0 0 X X X X X X X X X X X 0 0 0 0 0 0
T05    0 0 0 0 0 X X X X X X X X X X X 0 0 0 0 0 0
T06    0 0 X X X X X X X X X X X X X X X X X 0 0
T07    0 0 X X X X X X X X X X X X X X X X X 0 0
T08    0 0 X X X X X X X X X X X X X X X X X 0 0
T09    X X X X X X X X X X X X X X X X X X X X X
T10    X X X X X X X X X X X X X X X X X X X X X
T11    X X X X X X X X X X X X X X X X X X X X X
T12    X X X X X X X X X X X X X X X X X X X X X
T13    X X X X X X X X X X X X X X X X X X X X X
T14    X X X X X X X X X X X X X X X X X X X X X
T15    0 0 X X X X X X X X X X X X X X X X X 0 0
T16    0 0 X X X X X X X X X X X X X X X X X 0 0
T17    0 0 X X X X X X X X X X X X X X X X X 0 0
T18    0 0 0 0 0 X X X X X X X X X X X X X 0 0 0 0
T19    0 0 0 0 0 X X X X X X X X X X X X X 0 0 0 0
T20    0 0 0 0 0 X X X X X X X X X X X X X 0 0 0 0
T21    0 0 0 0 0 0 0 0 X X X X X X 0 0 0 0 0 0 0 0
T22    0 0 0 0 0 0 0 0 X X X X X X 0 0 0 0 0 0 0 0
C=
C=      1 2 3 4 5 6 7 8 9 0 1 2 3 4 5 6 7 8 9 0 1 2
C=
END
#####
NET     LT1  -29.17 -29.17 0.    20, 20
C=
C=      1 2 3 4 5 6 7 8 9 0 1 2 3 4 5 6 7 8 9 0
C=
T01    0 0 0 0 0 0 0 0 Y Y Y Y Y 0 0 0 0 0 0 0 0

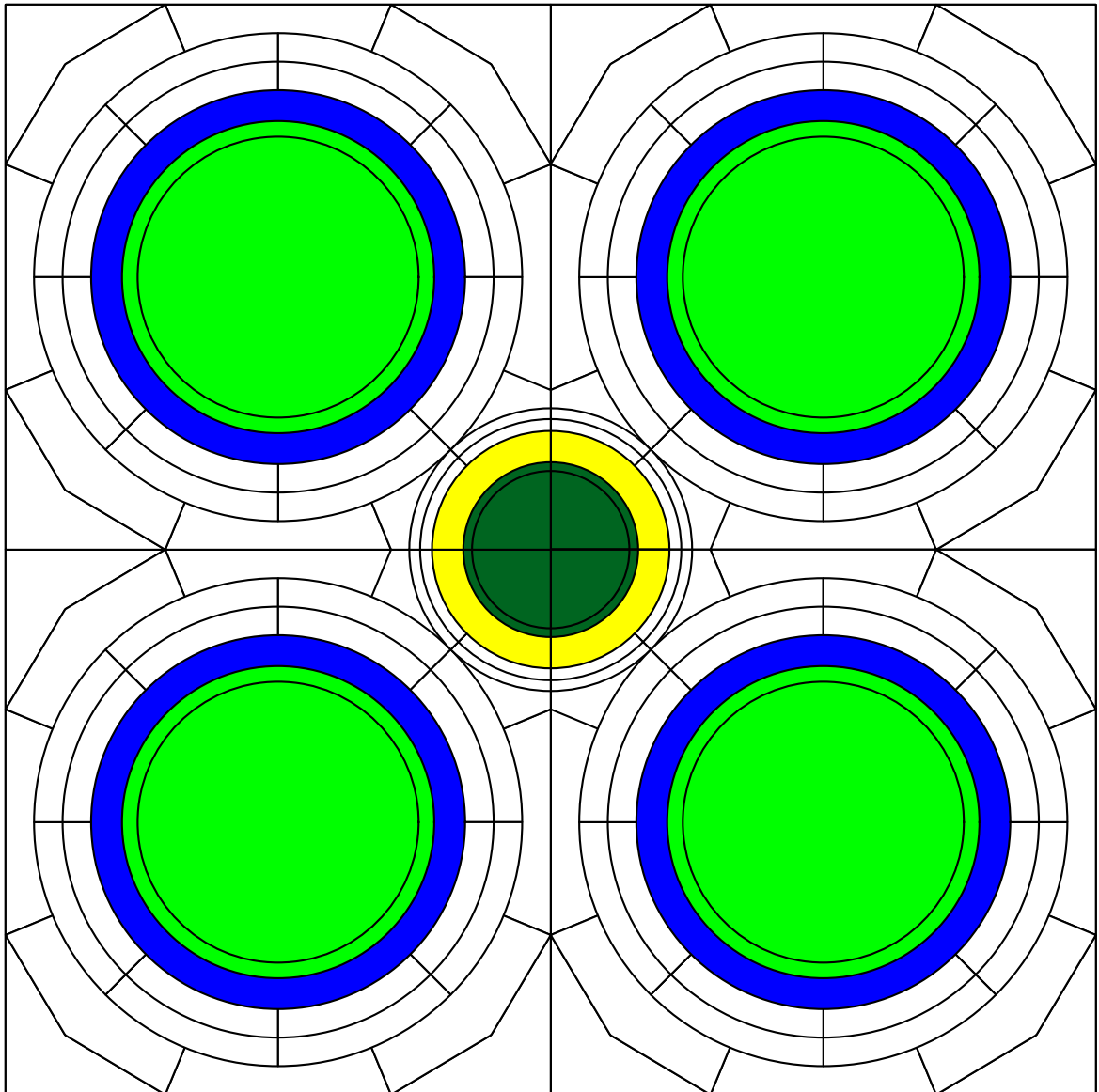
```

```

T02  0 0 0 0 0 Y Y Y Y Y Y Y Y Y Y 0 0 0 0 0
T03  0 0 0 Y Y Y Y Y Y Y Y Y Y Y Y 0 0 0
T04  0 0 Y Y Y Y Y Y 0 0 0 0 0 Y Y Y Y Y 0 0
T05  0 0 Y Y Y Y 0 0 0 0 0 0 0 0 0 Y Y Y 0 0
T06  0 Y Y Y Y Y 0 0 0 0 0 0 0 0 0 Y Y Y Y 0
T07  0 Y Y Y 0 0 0 0 0 0 0 0 0 0 0 0 Y Y Y 0
T08  Y Y Y Y 0 0 0 0 0 0 0 0 0 0 0 0 Y Y Y Y
T09  Y Y Y 0 0 0 0 0 0 0 0 0 0 0 0 0 0 Y Y Y
T10  Y Y Y 0 0 0 0 0 0 0 0 0 0 0 0 0 0 Y Y Y
T11  Y Y Y 0 0 0 0 0 0 0 0 0 0 0 0 0 0 Y Y Y
T12  Y Y Y 0 0 0 0 0 0 0 0 0 0 0 0 0 0 Y Y Y
T13  Y Y Y Y 0 0 0 0 0 0 0 0 0 0 0 0 0 Y Y Y
T14  0 Y Y Y 0 0 0 0 0 0 0 0 0 0 0 0 Y Y Y 0
T15  0 Y Y Y Y Y 0 0 0 0 0 0 0 0 0 Y Y Y Y 0
T16  0 0 Y Y Y Y 0 0 0 0 0 0 0 0 0 Y Y Y Y 0
T17  0 0 Y Y Y Y Y Y 0 0 0 0 0 Y Y Y Y Y 0 0
T18  0 0 0 Y Y Y Y Y Y Y Y Y Y Y Y Y 0 0 0
T19  0 0 0 0 0 Y Y Y Y Y Y Y Y Y Y 0 0 0 0
T20  0 0 0 0 0 0 0 Y Y Y Y Y Y 0 0 0 0 0
C=
C=    1 2 3 4 5 6 7 8 9 0 1 2 3 4 5 6 7 8 9 0
C=
END
FINISH NCG
SPNT  0.9, 0.9, 50.
FINISH SP
ENGR  0.
L
FINISH REG
NTOT  200
FINISH RUL
NAMVAR CRD01
MAXSER 1
DTZML 20
NPRI  200
REGZ  -1
FULL
FINISH ALL


```

Figure A.1. HELIOS model of the central absorber rod in the middle of the four central fuel rods



Appendix B
MEASUREMENT PROTOCOLS

B.1 Measurement of the enrichment of the oxide fuel pellets

SOCIETE INDUSTRIELLE DE COMBUSTIBLE NUCLEAIRE	F/D-EC/78.140				
	<u>ANNEXE N° 16</u>				
REPUBLIQUE FRANÇAISE COMMISSARIAT A L'ÉNERGIE ATOMIQUE CENTRE D'ÉTUDES NUCLÉAIRES DE GRENOBLE AVENUE DES MARTYRS 38 - GRENOBLE					
ADRRESSER LA CORRESPONDANCE : S.P. 22 CENTRE DU TRU 38041 GRENOBLE CEDEX	TEL. (76) 87-41-11 TELEF. U.E.A. 6. VIA GRENOBLE PARIS N° 90471				
SERVICE DE CHIMIE ANALYTIQUE DE GRENOBLE LABORATOIRE CENTRAL D'ANALYSE ET DE CONTROLE GF/MP	Monsieur MEUNIER S. I. C. N. B.P. n° 1 38113 VEUREY				
RÉFÉRENCE A RAFFERLER : n° SCAG/LCAC/77-549	F 77.767 ED/IC U 660 1/06/1977 GRENOBLE LE 14 Juin 1977				
OBJET : Affaire LAUSANNE	<div style="border: 1px solid black; padding: 5px; width: fit-content; margin: auto;"> ANNEXE N° 16 16 JUIN 1977 FABRICATIONS S.I.C.N. - VEUREY </div>				
Monsieur, Nous vous prions de bien vouloir trouver ci-dessous les résultats concernant l'échantillon n° 59 026-1 - UO ₂ fritté enrichi 1,80 % - DF 6029 - Lot 2050					
<table border="1" style="width: 100%; border-collapse: collapse;"> <thead> <tr> <th style="width: 60%;">²³⁵U % par rapport au poids total de métal</th> <th style="width: 40%;">P ppm/U</th> </tr> </thead> <tbody> <tr> <td style="text-align: center;">1,8060 ± 0,0007</td> <td style="text-align: center;">< 10</td> </tr> </tbody> </table>		²³⁵ U % par rapport au poids total de métal	P ppm/U	1,8060 ± 0,0007	< 10
²³⁵ U % par rapport au poids total de métal	P ppm/U				
1,8060 ± 0,0007	< 10				
La facture correspondante vous sera adressée par les Services Financiers du CEN-G.					
Veuillez croire, Monsieur, à l'assurance de nos sentiments distingués.					
 A. HUART					

B.2 Masses of the uranium oxide fuel rods

École Polytechnique Fédérale de Lausanne

Laboratoire de physique des réacteurs et de comportement des systèmes (LRS)

CROCUS : Chargement UO2

page : 1 sur 8

No	Poids (g)
4	914.8
5	915.1
10	914.8
11	915.7
22	919.8
26	918.0
27	917.9
29	915.4
32	918.2
35	916.5
37	919.0
40	916.3
45	915.7
49	914.5
51	917.7
53	918.2
56	919.4
60	918.3
62	915.4
63	917.2
67	918.8
69	915.7
70	914.2
71	914.7
74	914.7

No	Poids (g)
80	916.6
86	913.4
90	916.2
97	913.5
98	913.3
105	913.5
106	912.9
107	915.2
108	914.9
110	917.0
118	914.7
131	918.7
144	919.4
145	917.7
129	918.1
160	919.3
130	918.4
41	918.2
102	915.5
99	913.9
94	916.6
109	916.4
59	917.2
92	918.2
91	914.6

Nombre de Poids total	crayons :	50
	UO2 (grammes)	45819.4

No	Poids (g)
95	914.2
103	917.2
48	914.9
77	916.9
64	917.1
24	914.0
93	917.0
81	916.0
112	916.7
87	914.2
88	913.9
46	914.9
78	916.8
61	916.5
18	917.0
122	916.5
89	914.2
6	917.4
17	917.2
42	919.0
34	917.3
117	913.1
16	916.4
1	916.2
14	916.1

No	Poids (g)
114	915.5
2	918.8
52	917.9
58	914.0
116	912.6
120	915.6
115	913.4
197	917.1
137	919.0
134	918.4
185	918.4
174	917.8
138	916.0
127	917.6
168	917.3
157	914.7
191	915.4
156	917.0
30	916.9
151	919.1
183	920.1
184	920.2
196	920.1
19	917.2
190	918.8

Nombre de Poids total	crayons :	50
	UO2 (grammes)	45829.6

No	Poids (g)
188	916.6
189	916.7
187	916.8
186	919.0
158	912.3
136	917.7
54	919.7
139	918.7
140	919.2
159	918.3
162	919.1
163	920.0
150	918.4
153	919.5
192	915.7
193	919.1
195	920.8
194	920.1
182	918.7
133	917.5
142	919.7
143	919.4
125	917.9
172	916.2
9	915.2

No	Poids (g)
50	918.5
72	915.4
8	915.0
85	915.9
65	917.9
44	916.7
7	915.9
28	917.4
20	916.4
76	915.9
73	918.4
23	913.9
21	915.1
57	919.8
36	918.0
12	917.7
13	916.9
167	916.1
199	919.4
135	918.8
155	914.2
200	919.0
152	919.1
201	916.4
198	919.9

Nombre de	crayons :	50
Poids total	UO2: (grammes)	45880.0

No	Poids (g)
178	920.4
181	918.7
164	920.6
165	919.4
166	918.5
101	915.7
75	915.6
55	919.4
124	916.9
179	920.6
96	915.8
175	915.3
177	916.1
25	916.3
180	921.8
100	913.7
31	917.9
84	918.5
83	920.2
146	917.3
170	917.2
161	916.8
141	919.5
171	915.9
66	919.7

No	Poids (g)
239	916.6
241	916.6
43	920.8
240	918.6
242	916.3
234	914.5
237	916.1
231	919.1
207	919.1
217	916.5
210	915.7
232	919.0
236	916.7
212	915.6
203	918.9
220	917.1
113	916.9
206	920.5
104	913.5
39	919.0
82	918.6
253	918.6
259	917.1
154	916.0
3	917.6

Nombre de	crayons :	50
Poids total	UO2: (grammes)	45882.8

No	Poids (g)
255	916.4
257	915.8
256	916.2
252	918.5
251	917.5
260	916.8
254	918.8
277	915.1
276	917.4
275	913.5
274	913.8
270	917.2
269	917.2
268	917.0
267	917.8
226	918.1
228	920.2
230	912.0
247	919.1
250	918.9
225	919.8
221	919.0
222	919.1
224	917.7
245	916.9

No	Poids (g)
244	916.3
273	917.4
284	915.7
285	916.0
287	916.5
265	919.0
264	918.1
263	917.2
261	917.0
169	917.5
149	916.8
266	916.9
283	915.6
281	914.6
292	917.7
282	916.0
290	916.3
233	916.8
248	917.7
213	914.9
218	917.1
300	920.7
297	916.6
314	914.7
313	916.3

Nombre de Poids total	crayons :	50
	UO2 (grammes) :	45849.2

No	Poids (g)
312	916.1
311	916.6
309	916.4
308	917.5
307	915.5
306	913.2
305	915.7
303	918.6
301	918.9
298	916.8
296	916.7
238	916.3
215	917.1
123	916.9
121	915.6
126	915.7
173	915.9
148	916.9
128	916.0
176	917.1
147	914.7
111	916.4
119	917.5
291	915.7
204	917.4

No	Poids (g)
280	914.5
262	917.4
33	918.2
288	914.0
132	917.5
326	918.8
327	918.5
328	918.5
330	918.2
319	918.3
317	916.9
315	917.1
322	918.3
323	918.5
335	918.8
334	918.6
332	917.7
331	918.0
325	918.6
324	919.0
316	916.8
320	918.9
318	917.0
271	918.4
304	917.4

Nombre de Poids total	crayons :	50
	UO2 (grammes) :	45855.1

No	Poids (g)
278	915.1
302	923.1
216	916.3
211	916.1
214	917.8
258	919.2
289	916.4
38	917.9
15	916.3
310	916.5
299	917.5
227	916.3
295	914.8
223	914.2
79	915.0
209	918.2
205	917.1
279	914.6
336	918.2
272	917.4

No	Poids (g)
246	916.5
243	915.8
235	916.8
202	914.2
286	917.0
249	915.5
219	910.9
321	918.2
333	919.7
294	917.2
329	917.6
68	912.1
47	916.2
208	916.6
229	916.7
293	916.5

Nombre de	crayons :	36
Poids total	UO2 (grammes) :	32995.5

Page	Nombre	Poids (g)
1	50	45819.4
2	50	45829.6
3	50	45880.0
4	50	45882.8
5	50	45849.2
6	50	45855.1
7	36	32995.5

Nombre de crayons :	336
Poids total UO2 (grammes):	308111.6
Rapport Mu/Muo2 :	0.8815
Poids total U (grammes):	271600.4
Enrichissement :	0.018
Poids U-235 (grammes):	4888.8

B.3 Dimensions and masses of the metallic uranium fuel rods

École Polytechnique Fédérale de Lausanne

Laboratoire de physique des réacteurs et de comportement des systèmes (LRS)

CROCUS Chargement Um 176

page : 1 sur 6

No	Poids (g)	Haut. (mm)
2	4237	1001.0
3	4243	1001.0
4	4264	1001.0
5	4231	1000.2
6	4223	1000.6
7	4240	999.8
10	4249	1000.7
12	4248	1000.0
16	4250	1000.0
17	4233	999.7
20	4238	1000.7
21	4231	1000.2
23	4219	1000.0
24	4234	1000.4
25	4230	1001.0

No	Poids (g)	Haut. (mm)
28	4228	1000.5
31	4229	999.8
32	4220	1000.2
34	4265	999.6
37	4226	1000.3
38	4252	1000.0
39	4248	999.5
40	4261	1000.5
42	4221	1000.0
43	4243	1000.6
44	4239	999.5
45	4244	999.5
46	4248	999.5
49	4237	1001.0
50	4210	999.9

Nombre de Poids total U	crayons:	30
	(grammes):	127141.0

No	Poids (g)	Haut. (mm)
51	4222	1000.0
52	4247	999.9
57	4255	1000.7
60	4253	1000.7
61	4249	1000.4
63	4255	999.8
64	4258	1000.6
65	4268	1000.2
66	4256	1001.1
67	4261	1000.3
68	4237	999.8
69	4246	1001.2
70	4250	1000.2
71	4284	1000.0
72	4285	1001.7
73	4280	1001.0
74	4282	1001.0
75	4286	1000.7

No	Poids (g)	Haut. (mm)
77	4283	1001.0
78	4159	1000.2
79	4158	1000.2
80	4128	1000.2
81	4151	1000.2
82	4162	1000.2
84	4175	999.7
85	4172	1000.6
86	4230	1000.0
87	4221	1000.3
88	4226	1000.0
91	4237	1000.0
93	4170	1001.0
94	4226	999.7
95	4213	1000.2
96	4248	999.5
97	4249	1000.5
98	4236	1000.0
99	3993	1000.6

Nombre de	crayons :	37
Poids total U	(grammes):	156311.0

No	Poids (g)	Haut. (mm)
101	4246	1000.2
102	4238	1000.0
104	4243	1000.0
105	4241	1000.4
106	4237	1001.0
107	4252	1000.5
108	4248	1001.0
109	4245	1000.0
112	4240	1001.0
113	4241	1000.6
114	4228	1000.0
116	4231	1000.0
117	4239	1000.5
118	4248	1000.0
119	4244	1000.0
120	4246	1000.0
122	4253	1000.3
123	4253	1000.6
124	4244	1000.5
125	4246	1000.0

No	Poids (g)	Haut. (mm)
126	4264	1000.2
127	4252	1000.0
128	4241	1000.6
129	4252	999.8
130	4249	1000.2
131	4224	1000.4
132	4252	1000.0
133	4247	1000.3
134	4249	1000.3
135	4244	999.8
136	4227	1000.2
137	4252	1000.3
139	4246	1000.5
140	4241	1000.3
141	4233	1000.0
142	4247	1000.6
143	4254	1000.0
144	4244	1000.5
145	4241	1000.3
146	4246	1000.2
148	4243	999.7
149	4249	1000.7

Nombre de	crayons :	42
Poids total U	(grammes):	178260.0

No	Poids (g)	Haut. (mm)	No	Poids (g)	Haut. (mm)
151	4240	1000.3	176	4232	999.8
152	4241	1000.2	177	4254	1000.2
153	4244	1000.0	178	4249	999.6
154	4250	1000.6	179	4214	1000.2
155	4240	1000.6	180	4235	999.8
156	4235	1000.3	181	4230	999.8
157	4222	999.8	182	4243	1000.5
158	4232	1000.2	183	4228	999.8
159	4231	999.8	184	4246	1000.0
			185	4232	1000.2
161	4246	999.7	186	4269	1000.3
162	4220	999.8	187	4244	1000.2
163	4239	1000.3			
164	4241	1000.3	189	4228	1000.0
165	4250	1000.5	190	4261	999.8
166	4229	1000.3	191	4258	1000.2
167	4250	1000.0	192	4258	1000.2
168	4240	999.7	193	4249	1000.5
169	4250	1000.3			
170	4237	1000.0	195	4245	1000.0
171	4247	1000.0	196	4253	1000.0
172	4249	1000.0	197	4240	999.8
173	4233	1000.3	198	4244	1000.0
174	4266	1000.2	199	4252	1000.5
175	4228	1000.2			

Nombre de	crayons :	46
Poids total U	(grammes):	195124.0

No	Poids (g)	Haut. (mm)
201	4226	1000.5
202	4237	1000.0
204	4227	1000.2
205	4247	1000.2
206	4237	1000.2
207	4257	1000.0
208	4246	999.8
209	4230	999.7
210	4225	1000.3
211	4248	1000.2
212	4257	999.8
213	4234	1000.2
214	4265	1000.2
215	4253	1000.2
216	4251	999.8
217	4257	1000.2
218	4257	1000.0
219	4229	1000.2
220	4158	1000.2
221	4238	1000.3
222	4239	1000.4

Nombre de	crayons :	21
Poids total U	(grammes):	89018.0

Page	Nombre	Poids (g)
1	30	127141
2	37	156311
3	42	178260
4	46	195124
5	21	89018

Nombre de crayons:	176
Poids total U (grammes):	745854.0

Enrichissement :	0.00947
------------------	---------

Poids U-235 (grammes):	7063.2
------------------------	--------

Longueur totale (mm):	1.76039E+05
-----------------------	-------------

Longueur moyenne (mm) :	1000.222
-------------------------	----------

Masse linéique (g/mm)	4.2368680
-----------------------	-----------

Section (cm ²)	2.2698007
----------------------------	-----------

Masse volumique (g/cm ³)	18.666256
--------------------------------------	-----------

OECD PUBLICATIONS, 2 rue André-Pascal, 75775 PARIS CEDEX 16
Printed in France.